Design and Application of Wave-Absorbing Materials in Integrated Circuits

Huangyu Wu, Songmao Han, Jinwen Yang, Seemab Hussnain, Xiujuan Wang, Haibo Zeng* and Weijin Li*

MIIT Key Laboratory of Advanced Display Materials and Devices & Materials Physical and Chemical Research and Practice Center, College of Materials Science and Engineering, Nanjing University of Science and Technology, Nanjing 210094 P. R. China

Abstract: The relentless drive toward higher density, higher operating frequencies, and heterogeneous integration in integrated circuits (ICs) has exacerbated electromagnetic interference (EMI) issues. Conventional shielding materials suffer from high density, susceptibility to corrosion, and secondary pollution due to their reflection dominant mechanism. In response, this review focuses on electromagnetic wave absorbing materials as a core solution for IC electromagnetic protection. Key design strategies—including magnetic dielectric synergy, core shell architectures, three dimensional porous/network structures, and multilayer/gradient configurations—are systematically examined. Their synthesis via solution based coating, template methods, and additive manufacturing is also discussed. Furthermore, the integration of absorbing materials into advanced packaging technologies—wafer level packaging (WLP), 2.5D/3D packaging, and system in package (SiP)—is analyzed, highlighting the specific EMI challenges of each platform and the corresponding absorber deployment schemes. Despite significant progress, challenges remain in the precise fabrication of complex structures, compatibility with CMOS processes, and multi physics (electrical thermal mechanical) coupling under real operating conditions. Future efforts should focus on multi scale structural regulation, multifunctional integration (absorption packaging heat dissipation), and intelligent design to achieve lightweight, ultra thin, and dynamically tunable absorbers. This review aims to provide a comprehensive reference for the design and application of wave absorbing materials in next generation high performance integrated circuits.

Keywords: Wave-absorbing materials, Integrated circuits, Electromagnetic interference, Electronic packaging, Multilayer structure.

1. INTRODUCTION

Since the 21st century, the rapid advancement of information technology has significantly facilitated people's daily lives. Concurrently, integrated circuits have assumed a critical role across various domains such as technology and national defense. The capabilities for massive data transmission, storage, and processing are pivotal to national information security and development. As semiconductor technology has entered the nanometer-scale era, transistor dimensions continue to shrink. "More-than-Moore" approaches, realized through system-in-package (SiP) and 3D integration technologies, enable high levels of functional integration, markedly enhancing the performance and density of integrated circuits. Heterogeneous integration, which combines chiplets with different processes and functionalities into a single package, further optimizes the performance and cost of integrated circuits [1-3]. However, this rapid development of integrated circuits has also introduced new challenges.

The high-density layout and high-frequency operation of integrated circuits lead to intensified electromagnetic interference. Within the same package, digital and analog signals couple through parasitic capacitance and inductance, causing crosstalk and radiated interference. When signal frequencies exceed 1 GHz, the radiation loss from PCB transmission lines increases with the square of the frequency, significantly raising the difficulty of electromagnetic compatibility (EMC) design. In the millimeter-wave frequency band, the parasitic effects of devices and electromagnetic transmission characteristics are significantly influenced by temperature and electromagnetic field distribution, resulting in fluctuations in the amplitude and phase response of transceiver channels and exacerbating interference [4]. Meanwhile, three-dimensional integration leads to concentrated system heat sources and reduced spacing between components. This strengthens the coupling of power inductance and parasitic inductance, making the problem of radiated electromagnetic interference more severe [5].

Traditional electromagnetic shielding technologies predominantly rely on metal-based materials such as stainless steel, aluminum, and copper, as well as traditional wave-absorbing materials like ferrites. These materials generally exhibit high density and are prone to corrosion. For instance, metallic shields, due to their

*Address correspondence to these authors at the MIIT Key Laboratory of Advanced Display Materials and Devices & Materials Physical and Chemical Research and Practice Center, College of Materials Science and Engineering, Nanjing University of Science and Technology, Nanjing 210094 P. R. China
E-mail: wjli@njust.edu.cn, zeng.haibo@njust.edu.cn

Received on 26-04-2026 Accepted on 01-06-2026 Published on 09-06-2026

E-ISSN: 3110-9772/26

significant weight, struggle to adapt to the evolving demands for lightweight and miniaturized integrated circuits. Furthermore, corrosion over prolonged use leads to a degradation in shielding effectiveness. Their shielding mechanism predominantly relies on electromagnetic wave reflection, with some metallic materials exhibiting reflection coefficients exceeding 10 dB. The reflected electromagnetic waves can cause secondary electromagnetic pollution, interfering with the operation of nearby precision electronic components, which contradicts the requirements for green electromagnetic protection. In terms of broadband adaptability, traditional materials show notable shortcomings. For example, in high-frequency scenarios like 5G millimeter-wave applications, the hysteresis and eddy current effects in ferrites diminish, leading to a significant decline in absorption performance. This renders them incapable of meeting the broad-frequency shielding demands arising from the increasing operating frequencies of integrated circuits. Furthermore, traditional shielding materials lack flexibility and reparability. Metallic shields or rigid composite materials are difficult to adapt to emerging applications such as flexible electronics and wearable devices. Once damaged, they cannot be effectively repaired, resulting in increased maintenance costs. Their compatibility with advanced packaging processes like three-dimensional chip interconnects and heterogeneous integration is also insufficient. For example, in TSV (through-silicon via) based 3D packaging, traditional shielding materials fail to address the issue of close-range electromagnetic coupling between chiplets and may even exacerbate signal integrity losses [6, 7].

Compared with traditional electromagnetic shielding technologies, electromagnetic wave-absorbing materials offer significant advantages in electromagnetic protection for integrated circuits and across various applications. First, they efficiently suppress electromagnetic interference (EMI). Unlike metal-based reflective shielding, absorbing materials dissipate electromagnetic energy as heat through mechanisms such as dielectric loss and magnetic loss, thereby eliminating secondary contamination and cavity resonance caused by multiple reflections of reflected waves within enclosed package cavities [8]. Second, they enhance electromagnetic compatibility (EMC). By reducing high-frequency signal crosstalk, electromagnetic wave-absorbing materials can improve the electromagnetic immunity of GPIO ports in digital logic circuits, particularly in the critical 200–700 MHz frequency band, where they reduce the thermal-stress-induced drift amplitude of the immunity threshold [9]. Third, they meet the demands for lightweight and flexible solutions. Traditional metal shielding cans, characterized by high density and large volume, struggle to satisfy the requirements of emerging applications such as wearable devices and flexible electronics for lightweight, ultra-thin, and bendable packaging. In contrast, absorbing materials can achieve low density, ultra-thin profiles, and mechanical flexibility through thin-film fabrication and composite integration with flexible matrices [10, 11]. Fourth, they offer broadband absorption and frequency tunability. By tailoring material composition and microstructure design, absorbing materials can realize effective absorption over a wide frequency range, thereby accommodating the demanding electromagnetic protection requirements of 5G/6G communications at high and multiple frequency bands [12, 13]. Furthermore, absorbing materials can be integrated with multifunctional properties such as thermal conductivity and mechanical reinforcement, enabling the possibility of “absorption-encapsulation-heat dissipation” integrated designs. These advantages make absorbing materials an ideal candidate for addressing electromagnetic interference issues in advanced packaging. The remainder of this article will systematically review the electromagnetic interference challenges in integrated circuit packaging, as well as design strategies and synthesis methods of absorbing materials tailored for integrated circuits, aiming to provide meaningful insights for the application of absorbing materials in integrated circuits.

2. ELECTROMAGNETIC INTERFERENCE IN INTEGRATED CIRCUIT PACKAGING

As previously mentioned, electromagnetic wave-absorbing materials offer significant advantages such as broadband operation, light weight, and high-efficiency attenuation, providing important solutions for electromagnetic protection at both the chip and package levels. However, the practical application of wave-absorbing materials in integrated circuits depends not only on their intrinsic performance but is also closely tied to their integration methods, packaging processes, and system architecture. Therefore, how to achieve efficient and reliable integration of wave-absorbing materials at the packaging level constitutes a core challenge for enhancing the overall electromagnetic compatibility and reliability of the system. The following section will systematically explain advanced electronic packaging technologies closely associated with wave-absorbing materials, focusing on analyzing the basic principles, key processes, and integration characteristics of wafer-level packaging, 2.5D/3D packaging, and system-in-package, while also exploring their application potential and challenges in electromagnetic protection design.

2.1. Integration of Wave-Absorbing Materials in Wafer-Level Packaging

WLP (Wafer-Level Packaging) is an important component of modern advanced packaging technologies. It is an advanced semiconductor packaging technique where, after wafer fabrication is completed, numerous chips on the entire wafer are simultaneously packaged and tested before being diced into individual devices (Fig. **1**). The WLP process begins with a wafer. One of its core technologies involves fabricating a redistribution layer (RDL) on the wafer surface. Through wafer-level thin-film deposition, lithography, electroplating, and other processes, the RDL reconfigures the metal interconnects on the chip surface, "fanning out" the densely packed original bond pads at the chip edges and redistributing them to broader areas with looser pitches, thereby laying the foundation for external interconnections [14]. Subsequently, an under bump metallization (UBM) layer and solder bumps are formed on the terminal pads of the RDL, creating the electrical and mechanical interface for connection to external circuit boards. For the more structurally complex Fan-Out Wafer-Level Packaging (FOWLP), the process differs. It first requires dicing the wafer into individual chips. These known-good dies are then repositioned onto a temporary carrier at a specific pitch, and a molding process is used to form a new "reconstituted wafer." Subsequent RDL and bumping processes are then performed on this larger-area reconstituted wafer. This allows a single package to accommodate more input/output pins than the chip's own size, making it highly suitable for multi-chip integration.

Wafer-level packaging (WLP) achieves true chip-scale packaging by completing the encapsulation and testing processes before wafer dicing. However, its highly integrated structure introduces unique electromagnetic interference (EMI) challenges. The EMI issues in WLP primarily arise from parasitic effects in its key structural component—the redistribution layer (RDL)—and from noise coupling between adjacent chips. The RDL in WLP typically consists of multiple layers of metal interconnects, and these high-density routing lines exhibit significant parasitic inductance, capacitance, and resistance at millimeter-wave frequencies [15-17]. Such parasitic effects lead to increased signal delay, aggravated overshoot/undershoot, and simultaneous switching noise (SSN) on the power distribution network, thereby degrading signal integrity [18, 19].

The lack of backside electromagnetic shielding constitutes the second EMI issue in wafer-level packaging. In the die face-up fan-out wafer-level packaging (FOWLP) process, the chip is placed on a temporary carrier with its active side facing upward, leaving the backside exposed and protected only by a very thin layer of mold compound [20-22]. Although this design achieves extreme miniaturization, it renders the chip backside a vulnerable point for electromagnetic radiation. For instance, in a system-in-package (SiP) where multiple chips coexist in close proximity within a single package, radiation from the backside of one chip may couple directly into sensitive nodes of an adjacent chip, leading to intra-system EMI [23, 24]. This issue is particularly pronounced in mixed-signal systems: the backside radiation from a high-power digital chip can severely degrade the receiver sensitivity of a nearby RF chip. Furthermore, the backside radiation in WLP can directly cause package-level radiated emissions to exceed regulatory limits, preventing the product from passing EMC certification. Especially in high-frequency applications such as 5G millimeter-wave and Wi-Fi 6E/7, package radiation has become a major bottleneck for system-level EMC design [25, 26].

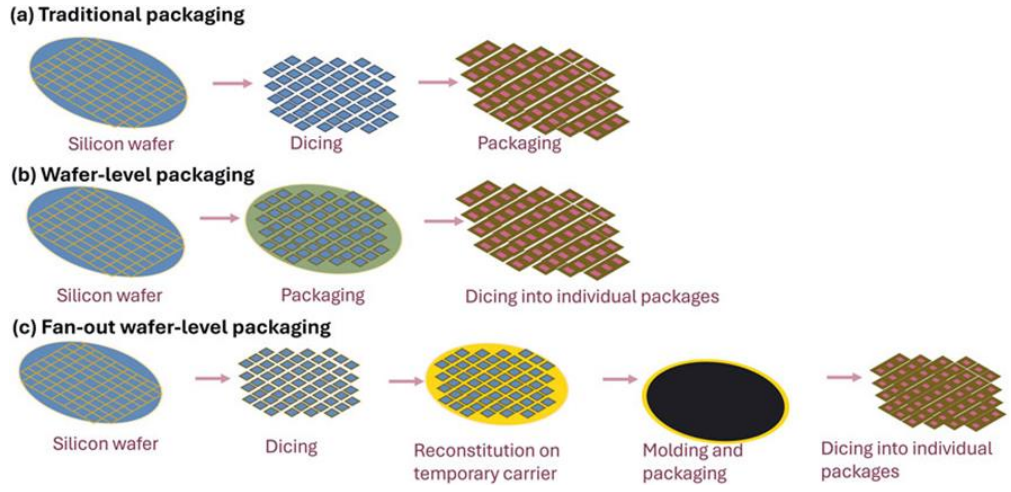

Figure 1: (A) Traditional packaging technology (B) Wafer-level packaging technology (C) Fan-shaped wafer-level packaging technology. Reproduce with permission [14]. Copyright, 2025 Frontiers in Electronics.

2.2. Integration of Absorptive Materials in 2.5D/3D Packaging Technologies

The core principle of 2.5D packaging lies in the insertion of an "interposer" with high-density interconnects between the chips and the package substrate. Multiple chips are mounted side-by-side on an interposer made of materials like silicon or glass. High-speed, high-bandwidth electrical interconnections between these chips are achieved through structures within the interposer, such as through-silicon vias (TSVs) or through-glass vias (TGVs), combined with its surface redistribution layers (RDLs), thereby integrating a compact system (Fig. **2**). In contrast, 3D packaging takes this a step further. It involves the direct vertical stacking and bonding of multiple chips using technologies like TSVs, enabling even shorter interconnect lengths, higher interconnect density, and more extreme spatial utilization [27].

The 2.5D packaging technology, based on silicon interposers and through-silicon vias (TSVs), begins its manufacturing process with the fabrication of the interposer itself. This involves creating a large number of vertical vias in a silicon wafer using techniques such as deep reactive-ion etching. Subsequently, insulating and barrier layers are deposited, and the vias are filled with copper via electroplating to achieve conductivity, thus forming the TSVs [28]. Following this, precise redistribution layer (RDL) networks are fabricated on both the front and back sides of the interposer using semiconductor thin-film processes, which serve for the fan-in and fan-out of chip signals. Tested and qualified chips are then precisely bonded to the surface of the interposer via flip-chip bonding, using micro-bumps with pitches as small as 40 micrometers. To reduce the overall package thickness, the wafer with the attached chips undergoes thinning—a common requirement is to reduce it below 100 micrometers—though this process can introduce issues such as wafer warpage. Finally, the entire structure is diced and mounted onto a larger organic package substrate to complete the connection with the external printed circuit board [29].

2.5D and 3D packaging technologies overcome the functional density limits of traditional 2D integration through vertical interconnects and three-dimensional stacking. However, the introduction of through-silicon vias (TSVs) and chip stacking also brings EMI issues that are distinctly different from those in WLP. In 2.5D packaging, TSVs within the silicon interposer are a key structure for vertical chip-to-chip interconnection [30-32]. Nevertheless, the large dimensions and dense arrangement of TSVs result in strong capacitive and inductive coupling between them. When high-frequency high-speed signals pass through TSVs, the vias themselves radiate electromagnetic waves into the interposer substrate, causing parasitic interference and fringe radiation. Crosstalk between adjacent signal TSVs thus becomes a central challenge in package EMC design. Capacitive coupling between TSVs originates from the parasitic capacitance between vias, through which displacement current couples into neighboring vias at high frequencies. Inductive coupling arises from mutual inductance between TSVs, where time-varying currents induce electromotive forces in adjacent TSVs [33, 34]. Crosstalk manifests as noise spikes on the victim line, which can lead to logic errors and timing violations. Signal integrity is worst when simultaneous, opposite-direction coupled transitions occur on the aggressor lines. At advanced technology nodes, shrinking noise margins mean that even weak electromagnetic coupling can cause logic errors and timing violations. Differential TSVs are often used for differential signal transmission in 3D integration, but they are also susceptible to electromagnetic field interference from adjacent signal/ground paths [35, 36].

The core of 2.5D packaging is the silicon interposer, whose electromagnetic properties have a decisive impact on system performance. On one hand, the finite resistivity of silicon leads to significant substrate losses for high-frequency signals. Finite-element simulation studies have shown that in the frequency range from 400 MHz to 20 GHz, the resistivity of the silicon interposer notably affects insertion loss, especially above 2.5 GHz, where free carriers in low-resistivity

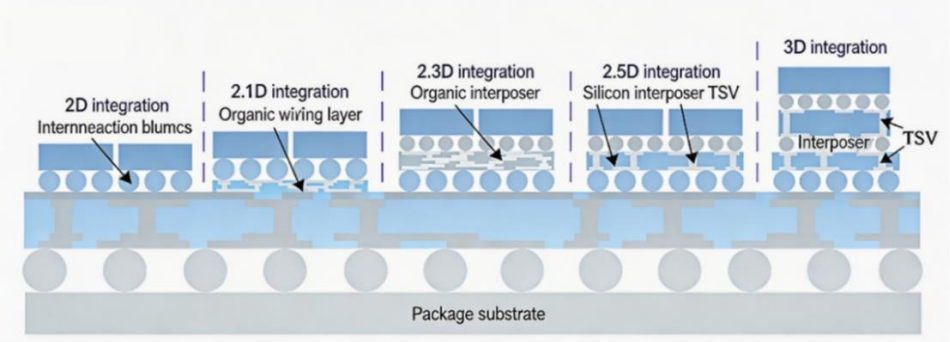

Figure 2: Schematic of multi-chiplet integration technology classification and structure.

silicon substrates absorb electromagnetic wave energy, causing signal attenuation. On the other hand, the interposer, together with the overlying and underlying chips, micro-bumps, and substrate, forms a complex electromagnetic cavity structure. When the cavity dimensions become comparable to the signal wavelength, cavity resonance amplifies the electromagnetic field intensity at specific frequencies, coupling into sensitive nodes and causing signal distortion [37, 38]. This issue is particularly prominent in 2.5D/3D packaging because the introduction of the vertical dimension increases the complexity of cavity modes.

In 3D packaging, TSVs are the core structure enabling vertical chip-to-chip interconnection, but their large dimensions and tight spacing also make them a major source of electromagnetic interference. The large size and close pitch of TSVs give rise to undesirable coupling capacitance between adjacent TSVs. This parasitic coupling causes mutual interference between neighboring TSVs and generates crosstalk noise, further threatening the reliability of inter-layer data transmission [39, 40].

2.3. Integration of Absorptive Materials in System-in-Package (SiP)

System-in-Package (SiP) technology represents a critical pathway for addressing the integration challenges of electronic systems in the post-Moore era. It is not a single technology but rather a comprehensive approach that integrates multiple functional chips, passive components, and even heterogeneous devices into a single package through high-density interconnects and packaging techniques, thereby forming a complete system or subsystem (Fig. **3**). In contrast to a System-on-Chip (SoC), which must integrate all functionalities onto a single die, the core principle of SiP lies in its "system-in-a-package" concept. It enables the interconnection and integration of pre-fabricated and tested mature chips, arranged either side-by-side in two dimensions or stacked in three dimensions, via high-density wiring on a substrate. This approach circumvents the process compatibility challenges inherent in single-chip integration [24, 41].

The fabrication of a complete SiP module begins with the design and processing of the substrate, which serves as the platform for mounting all components and establishing electrical interconnections. Materials such as silicon interposers, organic substrates, or ceramic substrates may be employed. The subsequent critical step involves chip attachment and interconnection. This core technological stage typically integrates two mainstream methods: wire bonding and flip-chip bonding. Wire bonding is a mature and cost-effective technique, whereas flip-chip bonding offers shorter interconnect paths, higher input/output (I/O) density, and superior electrical performance [42]. For more complex systems, three-dimensional stacking becomes an essential approach to enhancing integration density. This involves a series of precision processes, including chip thinning, via formation, and interlayer alignment and bonding. After component integration, encapsulation is performed to provide mechanical and environmental protection. Depending on application requirements, compartmentalized shielding or conformal shielding techniques may also be applied to suppress electromagnetic interference. Finally, through processes such as solder ball attachment or pin installation, a standardized, surface-mountable package is formed [43].

System-in-Package (SiP) integrates multiple heterogeneous chips and passive components within a single package, enabling a transition from chip-level integration to system-level integration. However, this

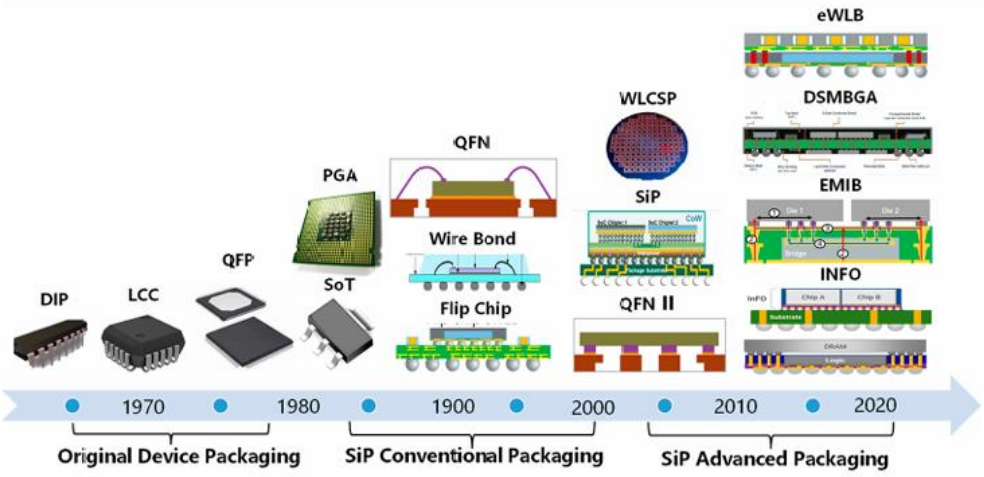

Figure 3: Trends in SiP. Reproduce with permission [24]. Copyright, 2023 MDPI.

integration paradigm introduces unique electromagnetic interference issues that are not present in WLP or 2.5D/3D packaging [44, 45]. As digital, analog, and RF functions become deeply integrated within SiP, and as chip-to-chip spacing shrinks to sub-millimeter scales, EMI exhibits a composite nature featuring multiple sources, multiple frequency bands, and multiple coupling paths. SiP dramatically reduces the distance between chips to enable high-speed, low-power interfaces, but this also means that the separation between noise sources and sensitive circuits is shortened to millimeter or even sub-millimeter levels. Consequently, the intensity and complexity of electromagnetic coupling far exceed those of traditional package forms.

One of the most distinctive features of SiP is the close coexistence of digital, analog, and RF circuits within a single package, which leads to serious self-interference issues. High-speed digital logic circuits become sources of EMI emission, while RF and analog circuits act as victims of EMI [46, 47]. When an RF receiver is integrated with digital functions in the same package, digital switching noise can overwhelm the RF signal, degrading receiver sensitivity. Meanwhile, even if unwanted energy from an RF transmitter is partially filtered at the output, it may still couple into the receive side through the limited isolation within the package, reducing the signal-to-noise ratio of the entire communication link. In SiPs that include switching mode converters, power integrity issues and voltage fluctuations on the power rails can severely interfere with the performance of sensitive analog devices embedded in the same package. As power devices continue to be miniaturized, switching frequencies increase and switching times shorten, generating significant high-frequency switching noise on the power rails [48, 49].

The package structure of SiP—comprising the substrate, mold compound, metal shielding lid, or heat spreader—forms a complex electromagnetic cavity. When the cavity dimensions become comparable to the wavelengths of the internal signals, standing wave patterns can develop at specific frequencies, leading to significant local amplification of the electromagnetic field. Moreover, simultaneous switching noise (SSN) is closely coupled with cavity resonance between the power and ground planes. The underlying mechanism is that SSN excites cavity resonance modes between the power and ground planes, thereby amplifying power supply noise in certain frequency bands and further coupling it into sensitive signal lines [19, 50]. In the assembly of RF system-in-package (RF SiP), although traditional metal cavity shielding can effectively suppress interference, it increases package thickness and weight. Conformal shielding, while enabling a thin profile, introduces reflection and cavity mode issues within the enclosed cavity. Thus, achieving effective EMI shielding while maintaining a small form factor remains a key challenge.

In summary, the various integration schemes for integrated circuits all give rise to electromagnetic interference issues such as crosstalk, cavity resonance, and TSV coupling, which have become critical factors limiting the performance and reliability of ICs. Traditional reflective shielding tends to induce secondary interference and cavity resonance, making it difficult to meet the demands of advanced packaging in terms of miniaturization, low profile, and wide high-frequency bandwidth. Therefore, investigating absorbing materials capable of efficiently dissipating electromagnetic waves, along with their underlying mechanisms, has become a core approach to addressing package-level electromagnetic compatibility challenges. The following sections will systematically elaborate on the fundamental concepts, loss mechanisms, and key performance requirements of absorbing materials for integrated circuits, and propose design strategies for developing absorbing materials that can efficiently dissipate electromagnetic waves.

3. OVERVIEW AND MECHANISM OF ABSORBING MATERIALS

3.1. Overview of Absorbing Materials

Wave-absorbing materials are a class of functional materials that can effectively absorb and attenuate incident electromagnetic waves. They convert electromagnetic energy into other forms of energy such as thermal or mechanical energy for dissipation, or reduce electromagnetic wave reflection through phase-cancellation interference. This capability serves to lower electromagnetic interference, ensure the stable operation of electronic equipment, and meet requirements for applications such as stealth technology and electromagnetic protection. These materials are typically composed of an absorber filler dispersed within a matrix material. Their core performance must satisfy criteria such as broadband effectiveness, high absorption rate, light weight, and suitability for specific application scenarios in terms of physical properties—such as flexibility, high-temperature resistance, and wear resistance [51, 52].

The core principle enabling wave-absorbing materials to achieve efficient absorption lies in ensuring effective electromagnetic wave incidence through impedance matching, followed by energy dissipation of the incident waves via electromagnetic loss, and finally suppression of the residual portion through destructive

interference. Together, these three processes form a complete chain of "incidence–dissipation–reflection cancellation," ultimately converting electromagnetic energy into harmless forms such as thermal energy for dissipation, thereby avoiding electromagnetic interference and secondary pollution (Fig. **4**). Impedance matching is the primary condition for wave-absorbing materials to function effectively. Its essence is to reduce the reflection of electromagnetic waves at the interface between air and the material by tailoring the material's electromagnetic parameters, thereby ensuring that electromagnetic waves smoothly enter the material's interior. The impedance characteristics of a material are jointly determined by its relative complex permittivity ($\varepsilon_r=\varepsilon'-j\varepsilon''$) and relative complex permeability ($\mu_r=\mu'-j\mu''$). The goal is to make the material's input impedance (Z_{in}) as close as possible to the wave impedance of free space [53]. The degree of matching is typically quantified by the impedance matching coefficient (M_z). When M_z approaches 1, interfacial reflection is minimized, and the incidence efficiency of electromagnetic waves is optimal. Simultaneously, to maximize the material's wave-absorbing capability, its electromagnetic loss capacity must be enhanced. Generally, larger values of complex permittivity and complex permeability can improve a material's electromagnetic loss capacity. However, this often leads to an imbalance in the material's impedance [54]. Therefore, the key to optimizing electromagnetic wave-absorbing materials lies in balancing impedance matching with electromagnetic loss capacity.

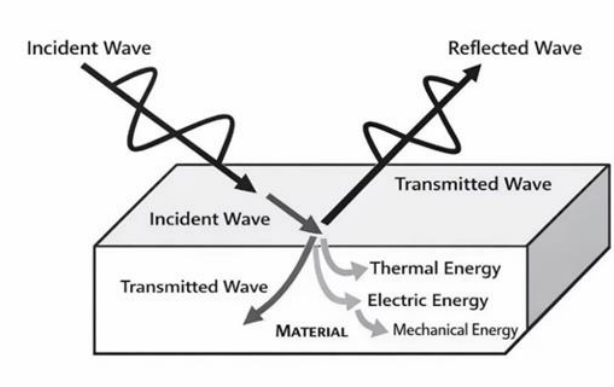

Figure 4: Principle of Electromagnetic Wave Absorption.

3.2. Microwave Loss Mechanism

Dielectric loss is one of the key mechanisms through which wave-absorbing materials convert electromagnetic energy into thermal energy for dissipation. It essentially involves energy loss resulting from processes such as charge polarization relaxation and carrier migration under the influence of a microwave electric field. This mainly includes polarization loss and conductive loss. Polarization loss dominates dielectric loss, originating from the alignment and relaxation of electric dipoles within the material under a microwave electric field. It can be specifically classified into electronic polarization, ionic polarization, orientation polarization, interfacial polarization, and defect-induced polarization. Significant differences exist in the polarization mechanisms across various material systems. Conductive loss, a specific form of dielectric loss, is fundamentally resistive loss. It refers to the process in which wave-absorbing materials with certain conductivity, under the action of a microwave electric field, allow internal carriers (electrons, holes) to move directionally, forming an electric current that converts microwave energy into thermal energy via the Joule effect. The conjugated π-electron system in conductive polymers provides a pathway for carrier delocalization, while heteroatom doping can further increase carrier concentration, enhance conductivity, and strengthen conductive loss [55, 56].

At microwave frequencies, the magnetic loss mechanisms of wave-absorbing materials primarily consist of eddy current loss and natural resonance loss. Eddy current loss originates from electromagnetic induction effects induced by alternating magnetic fields, while natural resonance loss relies on the resonant coupling between magnetic dipoles and the magnetic field. The synergistic interaction between these two mechanisms determines the wave-absorption performance of materials from microwave to millimeter-wave frequencies. Eddy current loss is the energy dissipation process in which a wave-absorbing material generates circulating currents via electromagnetic induction in an alternating magnetic field environment, converting the energy into Joule heat. According to the law of electromagnetic induction, when an alternating magnetic field penetrates a magnetic material, closed-loop currents perpendicular to the magnetic field direction form inside the material. These currents dissipate energy due to the material's electrical resistance. The loss intensity can be quantitatively described by the formula $C_0=\mu''(\mu')^{-2}f^{-2}$, where C_0 is the eddy current loss coefficient, μ' and μ'' are the real and imaginary parts of the complex permeability, respectively, and f is the magnetic field frequency [57-59]. Natural resonance loss is a strong energy absorption phenomenon that occurs in magnetic wave-absorbing materials when the natural precession frequency of magnetic dipoles (or magnetic domains) matches the frequency of the applied alternating magnetic field [60]. In the microwave frequency range, natural resonance significantly affects the permeability and loss characteristics of wave-absorbing materials.

Conductive loss is a physical process in which dielectric materials, under the influence of an

alternating or direct current electric field, experience directional migration of internal charge carriers, forming a leakage current that converts electromagnetic energy into thermal energy through Joule heating. As a core component of dielectric loss, it is widely present in various dielectrics including gases, liquids, and solids. At the heart of conductive loss lies the energy dissipation process of "carrier migration – Joule heat conversion." No dielectric is a perfect insulator; the directional movement of a small number of free charge carriers within it under an electric field forms a leakage current. According to Joule's law, as this current passes through the material's resistance, heat is generated, leading to the dissipation of electromagnetic energy [61].

In wave-absorbing materials, destructive electromagnetic interference refers to the coherent interaction between the wave reflected from the material surface and the wave that enters the material, is reflected back by the underlying metal substrate, and re-emerges. When these two waves meet the conditions of equal amplitude and a phase difference of π, they cancel each other out due to interference, thereby significantly reducing or eliminating electromagnetic wave reflection [62]. To achieve effective destructive interference, the thickness of the material is typically designed precisely to be one-quarter of the target wavelength or its odd multiples. This ensures that the wave reflected from the bottom of the material and the wave directly reflected from the surface acquire a half-wavelength path difference, introducing a 180° phase shift and making the two waves nearly equal in amplitude but opposite in phase. This classic design principle based on interference was first embodied in the Salisbury screen, a structure consisting of a thin absorbing layer coated on a metal substrate. However, such interference-based wave-absorbing materials also exhibit certain limitations, primarily characterized by a relatively narrow absorption bandwidth and a rapid degradation in absorption performance as the angle of incidence of the electromagnetic wave increases [63].

4. DESIGN AND SYNTHESIS OF ABSORBING MATERIALS FOR INTEGRATED CIRCUITS

Traditional electromagnetic wave absorbing materials are mainly divided into two categories: dielectric loss type and magnetic loss type. Dielectric loss materials typically exhibit a high complex permittivity and good high-temperature stability, but their complex permeability is close to unity, resulting in poor impedance matching; consequently, a large portion of electromagnetic waves is reflected at the surface and hardly enters the material interior. Magnetic loss materials, although capable of achieving strong absorption through mechanisms such as hysteresis loss, eddy current loss, and natural resonance, suffer from high density, susceptibility to oxidation and corrosion, and are limited by the Snoek limit, which causes a sharp decrease in permeability above the GHz range, leading to a limited absorption bandwidth. Performance optimization of traditional absorbing materials often focuses on enhancing a single loss mechanism—for example, increasing the filler content to raise permittivity or permeability—but this exacerbates impedance mismatch, significantly increases density, and degrades mechanical properties, making it difficult to simultaneously meet the comprehensive requirements of “thin, light, wide, and strong.” For application scenarios in integrated circuit packaging, absorbing materials face even more stringent constraints [64, 65]. First, the internal space of advanced packaging is extremely limited; the gap between the chip and the package substrate is typically only tens to hundreds of micrometers, requiring the absorber thickness to be controlled at the sub-millimeter or even micrometer scale. Second, with the development of high-frequency applications such as 5G/6G communication and millimeter-wave radar, operating frequencies have extended to tens of gigahertz and even the millimeter-wave band, demanding that absorbing materials maintain stable and efficient absorption performance over an ultra-wide bandwidth. Third, the high density of integration leads to a sharp increase in heat flux, so absorbing materials must also possess good thermal conductivity to avoid the impact of local hot spots on chip reliability. Furthermore, packaging processes impose strict requirements on mechanical flexibility, adhesion, and compatibility with CMOS technology [66-68]. Traditional single-component or simple physically blended absorbing materials are no longer sufficient to meet these multiple demands.

Traditional solutions mainly include metallic enclosures (copper, aluminum, steel cans) and ferrite tiles. Their operating mechanism is primarily reflection—incident waves are reflected rather than dissipated. This leads to several inherent drawbacks: first, secondary electromagnetic pollution, as reflected waves can couple into nearby components or excite cavity resonances; second, thickness and weight—metal cans typically exceed 0.5 mm in thickness with high areal density (e.g., copper ~8.9 g/cm³), while ferrite tiles are often >3 mm thick and brittle; third, narrow effective bandwidth—ferrites suffer from a sharp drop in permeability above several gigahertz, while metal shields offer high shielding effectiveness (>30 dB) only over limited frequency ranges; and finally, metal production and etching generate substantial waste and energy consumption. In contrast, the modern wave-absorbing materials

discussed herein operate on absorption through dielectric loss, magnetic loss, interfacial polarization, or their synergy, and offer several unique advantages. These include no secondary reflection pollution—electromagnetic energy is converted into heat, eliminating cavity resonance issues; significantly reduced thickness and weight—many designs achieve effective absorption (RL < −10 dB) at sub-millimeter to a few millimeters thickness; more importantly, through compositional and structural engineering, broadband and tunable performance can be achieved, with effective absorption bandwidths exceeding 30 GHz—for example, the PNIPAM gel achieves an effective absorption bandwidth of 34.96 GHz; and finally, modern absorber designs are more aligned with green manufacturing needs, as demonstrated by water-based inks, bio-derived precursors, and low-temperature solution processing, which have a lower environmental impact compared to metal etching [69, 70].

Therefore, the design of absorbing materials for integrated circuits must break away from traditional paradigms and pursue new routes based on multicomponent synergy and multiscale structural regulation. In recent years, researchers have carried out extensive work around the concept of composite multidimensional design, achieving notable progress in broadband absorption, ultra-thin thickness, light weight, and integration of thermal conductivity with wave absorption. The following sections will systematically review the design strategies of absorbing materials for integrated circuits from four perspectives: magnetic-dielectric synergistic composites, core–shell structures and surface engineering, three-dimensional porous/network structures, and multilayer/gradient structures.

4.1. Magnetic-Dielectric Synergistic Composite

The design of wave-absorbing materials for integrated circuits fundamentally involves finding an optimal balance among contradictory performance requirements and achieving performance breakthroughs through multi-component synergy and the construction of hierarchical structures. In the design of wave-absorbing materials for integrated circuits, the magnetic-dielectric synergistic composite strategy is key to realizing broadband absorption, strong attenuation, and ultrathin thickness. This strategy involves combining magnetic loss units and dielectric loss units at the microscopic scale to construct a hierarchical, multi-mechanism synergistic loss system, thereby addressing the complex electromagnetic environment within chips.

Regarding the strategy of multi-mechanism synergy between magnetic loss and dielectric loss units at the microscale, Zhang *et al*. [71]. employed a high-entropy oxide$(CoCrFeCuNi)_3O_4$ as the magnetic loss unit. The lattice distortion induced by its multi-principal-element characteristics provides a structural basis for enhancing dielectric polarization loss. This was further optimized through an elemental substitution strategy using Cu to replace Mn—Cu, as an active element, induces more significant lattice distortion and oxygen vacancies. This enhances dipole polarization while avoiding the magnetic weakening associated with traditional Mn-based materials, thereby achieving synergistic enhancement of dielectric and magnetic loss along with optimized impedance matching. Furthermore, a core-shell heterostructure was constructed at the microstructural level. The intermediate carbon shell acts as an "impedance matching bridge," forming a stepped impedance transition layer of "air–graphene–carbon shell–HEO core." This effectively suppresses surface reflection and guides electromagnetic waves into the structure. The introduction of graphene builds a three-dimensional conductive network, which strengthens conductive loss while the heterogeneous interfaces between graphene and the core-shell particles induce intense interfacial polarization. Ultimately, a multi-level synergistic loss system is formed: the HEO core broadens the magnetic resonance frequency band through multi-magnetic-ion coupling, while the carbon shell and graphene network jointly contribute to interfacial polarization, dipole polarization, and conductive loss, enabling the magnetic-dielectric synergistic composite loss mechanism to operate cooperatively across the core–shell–network multi-scale (Fig. **5**). Through composition and structural regulation, this design achieved an effective absorption bandwidth of 4.9 GHz at an ultra-thin thickness of 1.6 mm and a strong reflection loss of -60.9 dB at 2.0 mm. Its compatibility with 3D printing processes demonstrates potential for integration in integrated circuit packaging The multi-principal-element lattice distortion and oxygen vacancies in the high-entropy oxide core serve as atomic-scale dipole polarization centers, enhancing polarization loss. On one hand, the substitution of Cu for Mn further increases lattice disorder while preserving the magnetic moment, thereby promoting dipole polarization. On the other hand, the carbon shell plays a dual role: it suppresses eddy currents and constructs a stepped impedance transition of “air–graphene–carbon shell–HEO core”, reducing surface reflection. Consequently, this hierarchical architecture achieves cross-scale synergistic loss involving dipole polarization, interfacial polarization, and conduction loss, while simultaneously optimizing impedance matching and attenuation capability.

Compared with conventional single-mechanism absorbers, the magnetic-dielectric synergistic design

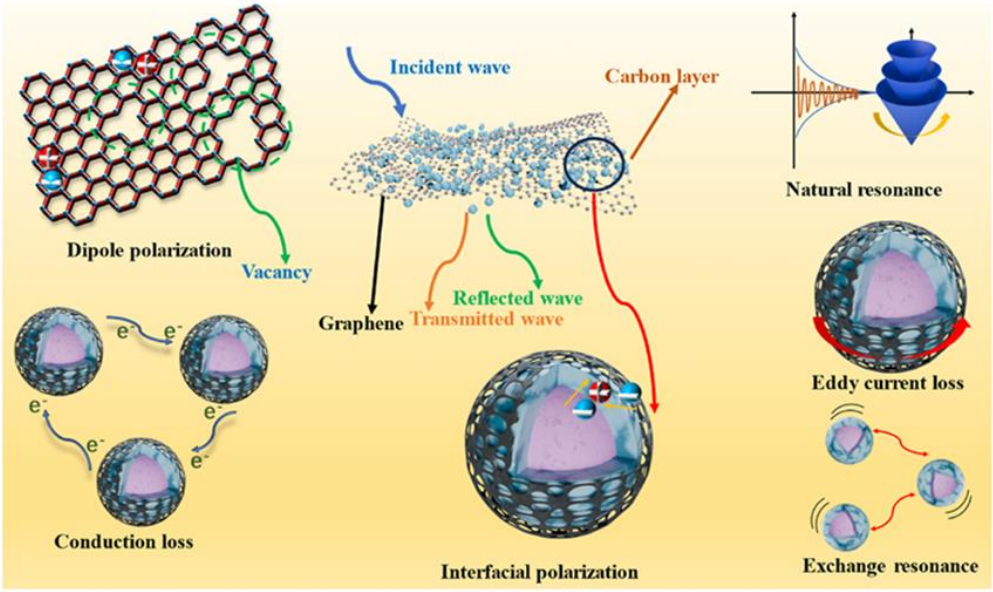

Figure 5: Schematic diagram of microwave absorption mechanism of composite materials. Reproduce with permission [71]. Copyright, 2025 Elsevier.

exhibits distinct advantages. Traditional magnetic-loss materials, such as ferrites and carbonyl iron, suffer from high density, eddy current degradation above several gigahertz, and a sharp permeability drop due to the Snoek limit, resulting in a narrow effective bandwidth. In contrast, single dielectric-loss materials like carbon black and graphene typically possess high permittivity but exhibit poor impedance matching with free space, leading to strong surface reflection rather than absorption. The work by Zhang *et al*. overcomes these limitations by integrating a high-entropy oxide magnetic core with a carbon/graphene dielectric network, achieving broadband response and strong absorption at sub -2 mm thickness.

In parallel, Shu *et al*. [72]. fabricated multilayer MXene with abundant surface functional groups via an etching method, resulting in a negatively charged surface. Meanwhile, uniformly sized $CoFe_2O_4$ nanospheres were synthesized using a high-temperature solvothermal method and subsequently treated with cetyltrimethylammonium bromide to impart a positive surface charge. Leveraging the electrostatic attraction between opposite charges, the researchers anchored $CoFe_2O_4$ particles uniformly onto the surfaces and interlayers of MXene, thereby forming a three-dimensional hybrid structure with abundant heterointerfaces. In this configuration, MXene provides a highly conductive network and contributes to dielectric loss, while its surface functional groups and structural defects induce dipole polarization and interfacial polarization. Simultaneously, $CoFe_2O_4$ introduces magnetic loss mechanisms such as hysteresis loss, natural resonance, and exchange resonance, and its interfacial coupling with MXene enhances magnetic anisotropy. Compared with single-component magnetic absorbers (e.g., pure $CoFe_2O_4$), the magnetic-dielectric synergistic design significantly improves impedance matching and broadens the effective absorption bandwidth. In this work, positively charged $CoFe_2O_4$ nanospheres were loaded onto negatively charged MXene layers via electrostatic assembly to construct a three-dimensional heterostructure. This structure exhibits two key features: first, abundant $CoFe_2O_4$/MXene heterointerfaces, which generate strong Maxwell-Wagner polarization due to the significant conductivity contrast between semiconducting $CoFe_2O_4$ and metallic MXene; second, the layered morphology of MXene provides a two-dimensional conductive network that facilitates conduction loss, while its surface terminations (–O, –OH, –F) introduce additional dipolar relaxation centers. The magnetic $CoFe_2O_4$ contributes natural resonance and exchange resonance losses, and synergistically interacts with the dielectric response of MXene to broaden the effective absorption frequency range.

However, this strategy faces two critical trade-offs: First, increasing the dielectric loss component (e.g., MXene or graphene) enhances attenuation but raises electrical conductivity, which may cause eddy current loss and degrade high-frequency performance above 18 GHz. Second, uniform dispersion of magnetic nanoparticles in a dielectric matrix remains challenging; agglomeration leads to local impedance mismatch and reduced absorption efficiency. Therefore, for integrated circuit packaging operating in the 5G millimeter-wave band (24–40 GHz), magnetic-dielectric composites require precise control of filler morphology and volume

fraction—typically below 20 wt%—to balance loss and matching.The above work demonstrates that the magnetic-dielectric synergistic composite strategy, by rationally integrating magnetic loss units and dielectric loss units at the micro-/nano-scale, can effectively reconcile the inherent trade-off between impedance matching and electromagnetic loss. This strategy not only broadens the effective absorption bandwidth and reduces the matching thickness, but also offers the flexibility to incorporate additional functionalities such as thermal conductivity and printability. For integrated circuit packaging applications, where space is extremely limited and heat dissipation is critical, such synergistic designs provide a promising pathway toward ultra-thin, light-weight, high-performance absorbing materials that are compatible with advanced packaging processes.

4.2. Core-shell Structure and Surface Engineering

Core-shell structures and surface engineering serve as effective strategies in functional material design, demonstrating significant potential in addressing the synergistic challenges faced by wave-absorbing materials for integrated circuits, such as low electrical conductivity, chemical stability, and high loss intensity. Through ingenious core-shell structure design and surface modification, precise regulation of material conductivity, chemical stability, and electromagnetic wave loss capability can be achieved, meeting the stringent requirements of integrated circuits for wave-absorbing materials. A core-shell structure typically consists of a core material and an outer shell layer. By rationally selecting core-shell components and tuning structural parameters, the electromagnetic properties and surface chemical characteristics of the material can be optimized. Commonly used insulating shell materials include SiO_2, Al_2O_3, polymers such as polyaniline and polypyrrole, and nitrides like Si_3N_4. These materials possess wide bandgap characteristics and high electrical resistivity, effectively limiting carrier migration and reducing the overall electrical conductivity of the material.

A representative implementation of core–shell design for integrated circuit applications was reported by Zheng *et al*. [73], who synthesized Fe–Co alloy nanoparticles as magnetic cores via a chemical reduction method. A silica dielectric layer was then coated onto the particle surfaces using a sol–gel process to form a FeCo@SiO_2 core–shell structure. Finally, a polyaniline (PANI) conductive polymer layer was deposited on the outer surface through in-situ polymerization, yielding a complete FeCo@SiO_2@PANI triple-layered core–shell configuration. In this architecture, the Fe–Co alloy core provides magnetic loss mechanisms, including hysteresis loss and natural resonance. The intermediate SiO_2 layer serves as a dielectric material that modulates the permittivity, optimizes impedance matching, and acts as a protective barrier to prevent oxidation and agglomeration of the Fe–Co alloy. The outer PANI layer, as a conductive polymer, introduces abundant dipole polarization and interfacial polarization, while enhancing conduction loss through its conductive network. The test results show that at a filler loading of 20 wt% and a matching thickness of 2.9 mm, the composite achieves a minimum reflection loss of –69.5 dB and an effective absorption bandwidth of 8.6 GHz (Fig. **6** c,f,i). The triple-layer FeCo@SiO_2@PANI structure decouples impedance matching from loss mechanisms. The intermediate SiO_2 layer reduces the effective permittivity, alleviating the impedance mismatch problem of bare FeCo nanoparticles, while electrically isolating adjacent magnetic cores to suppress eddy currents. The outer PANI shell not only constructs a conductive network to enhance conduction loss, but its polar –NH– groups also contribute to dipole polarization. The two heterointerfaces (FeCo/SiO_2 and SiO_2/PANI) generate independent Maxwell-Wagner relaxation processes, with the respective shell thicknesses determining the relaxation times. Finally, increasing the thickness of the SiO_2 layer shifts the low-frequency absorption peak to even lower frequencies, thereby achieving tunable absorption. This triple-layer core–shell structure exhibits marked improvements over conventional single-component or bilayer absorbers. Relative to pure magnetic cores, the SiO_2 intermediate layer effectively suppresses eddy currents and oxidation, while the outer PANI shell enhances dielectric loss and impedance matching. Compared with single dielectric absorbers, the magnetic core provides additional low-frequency magnetic loss, broadening the effective absorption bandwidth to 8.6 GHz.

In another effort exploiting the dual role of a ceramic shell, Liang *et al*. [74] employed Si_3N_4 as the shell material for a graphene core, constructing a DG/Si_3N_4 multi-layer alternating core-shell nanowire film through chemical vapor deposition. The Si_3N_4 shell serves both as an impedance matching layer to optimize electromagnetic wave incidence and as a protective layer inhibiting oxidation of the graphene core. Concurrently, its inherent high resistivity ensures low electrical conductivity of the material, achieving a strong reflection loss of -77.3 dB and a wide absorption bandwidth of 7.44 GHz. In the DG/Si_3N_4 nanowire film, the ceramic Si_3N_4 shell possesses a low permittivity ($\varepsilon' \approx 4$–6), which reduces the effective permittivity of the composite and brings the input impedance close to that of free space ($Z \approx 377\ \Omega$). Its high electrical resistivity (>$10^{12}\ \Omega\cdot$cm) suppresses conduction loss, making

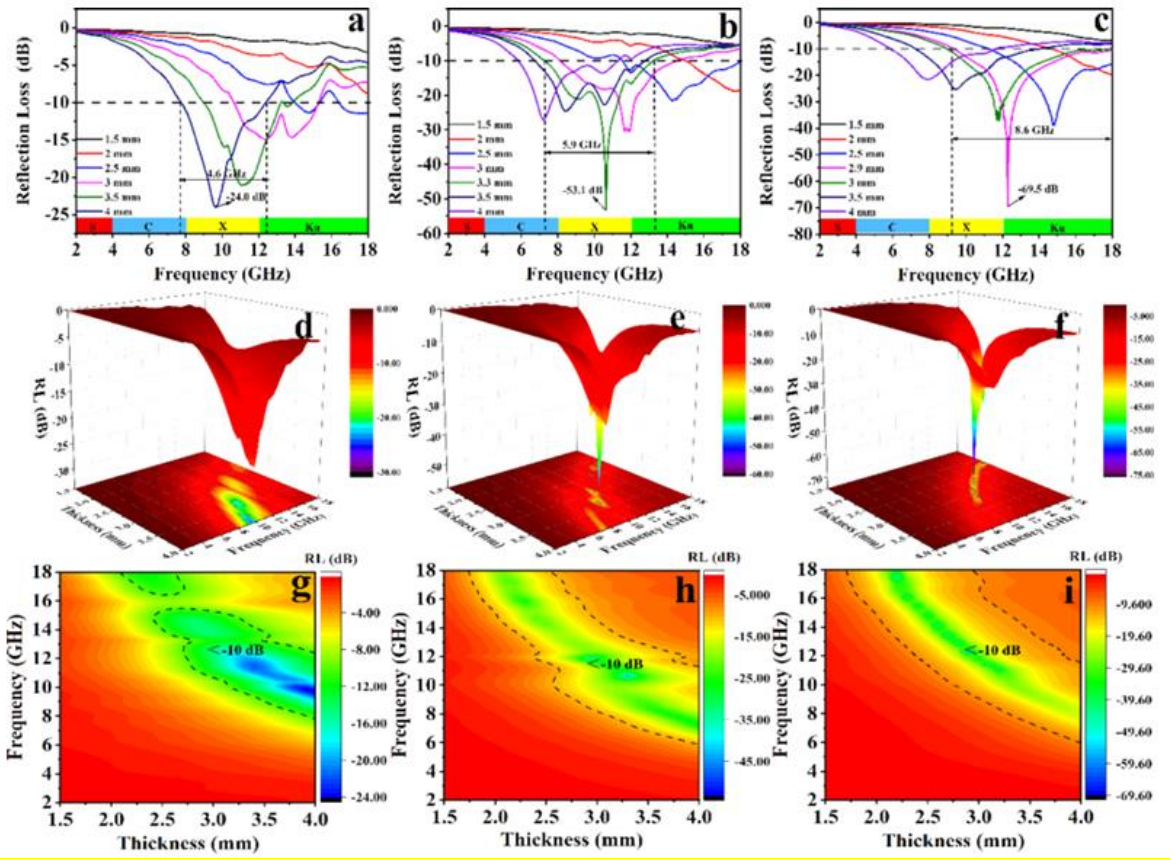

Figure 6: The RL, 3D plots and 2D projections with various thicknesses of FeCo (a, d, g), FeCo@C (b, e, h) and FeCo@C@BDC (c, f, i) with different thickness [73]. Copyright, 2023 Elsevier.

interfacial polarization the dominant mechanism. The alternating graphene/Si_3N_4 interfaces form a high density of heterojunctions, each contributing to charge accumulation and relaxation. Since this all-dielectric design contains no magnetic components, it avoids eddy current losses, thereby explaining its stable performance up to 18 GHz. This ceramic-shell design offers distinct advantages over conventional carbon-based absorbers and magnetic materials. Pristine graphene or carbon nanotubes typically suffer from excessively high conductivity and poor impedance matching, leading to strong reflection rather than absorption. In contrast, the Si_3N_4 shell in Liang's work effectively reduces the effective permittivity of the composite, acting as an impedance matching transformer that allows more electromagnetic waves to enter the structure. Furthermore, unlike magnetic absorbers that experience a sharp decline in permeability above several gigahertz due to the Snoek limit, this all-dielectric design maintains stable performance in the high-frequency range. The Si_3N_4 shell also provides oxidation resistance, addressing the poor thermal stability of graphene in air—a critical advantage for packaging processes involving high-temperature steps such as solder reflow.

Extending this concept to multifunctional protection, Liu *et al*. [75] developed multifunctional hollow carbon microspheres that achieve a dual-passivation anti-corrosion effect through surface ZnO conversion and layered double hydroxide (LDH) formation. The material surface exhibits electronegativity, reducing the adsorption/accumulation of corrosive ions like Cl^- and OH^- on the substrate through electrostatic repulsion. Furthermore, as immersion time increases, magnetic particles transform into LDHs, which further prevent corrosive ions from approaching the substrate surface via their strong anion capture capability, thereby realizing long-term anti-corrosion performance. The hollow carbon microsphere provides a lightweight structural framework with a high specific surface area. The ZnO/LDH dual passivation layer not only serves as corrosion protection but also acts as an additional polarization source: on one hand, the electronegative LDH surface creates a built-in electric field that enhances dipole polarization; on the other hand, the ZnO/carbon interface contributes to interfacial polarization. However, magnetic particles (e.g., Fe, Co) gradually transform into non-magnetic LDH over time, leading to a progressive loss of magnetic loss contribution. This multifunctional hollow carbon microsphere design addresses a key shortcoming of conventional absorbing materials—corrosion susceptibility. Traditional magnetic absorbers are prone to oxidation and galvanic corrosion in humid or saline environments, leading to rapid degradation of both

magnetic loss capability and structural integrity. Pristine carbon-based absorbers, while chemically more stable, often lack active corrosion protection and suffer from poor impedance matching due to excessively high conductivity. Liu *et al*. constructed a ZnO/LDH dual-passivation layer on hollow carbon microspheres, providing active corrosion resistance: the electronegative surface repels corrosive anions, while the LDH transformation over time further captures Cl^- and OH^- via ion exchange. This offers new insights and approaches for the design of durable absorbers for harsh-environment electronics.

Wang *et al*. [76] prepared four composite materials—SCNT-CuHT, DCNT-CuHT, MCNT-CuHT, and HCNT-CuHT—by growing CuHT onto the surfaces of different types of carbon nanotubes via an in situ polymerization method. The morphology and structure of the composites were characterized using techniques such as SEM, TEM, XRD, and FT-IR, while their electromagnetic parameters were measured with a vector network analyzer over the 2–18 GHz frequency band. The study highlights that by constructing an interfacial-engineered one-dimensional/two-dimensional heterostructure and selecting carbon nanotubes with distinct structures, the absorption performance can be precisely tuned for specific frequency bands, thereby achieving a significant enhancement in electromagnetic wave absorption properties. Wang *et al*. directly grew the conductive metal-organic framework CuHT onto the surface of carbon nanotubes (CNTs), constructing a one-dimensional/two-dimensional heterostructure. In this structure, the CNTs provide a highly conductive backbone, while the CuHT shell introduces additional polarization centers through its metal-organic coordination bonds. By selecting CNTs with different morphologies, the electrical conductivity of the composite can be tuned, thereby affecting the percolation threshold and the density of CNT/CuHT interfaces. A higher interface density shifts the relaxation peak to lower frequencies, enabling frequency-selective absorption. Compared with conventional single-component or physically blended absorbers, traditional carbon nanotube (CNT) absorbers, while providing conductive loss, typically suffer from excessively high permittivity and poor impedance matching. In contrast, pure metal-organic frameworks (MOFs) such as CuHT often exhibit low electrical conductivity and limited dielectric loss. By growing CuHT directly onto CNT surfaces, Wang *et al*. constructed a one-dimensional/two-dimensional hetero-structure that introduces abundant heterogeneous interfaces, promoting interfacial polarization while moderating the overall permittivity. Furthermore, the ability to tune the absorption performance by selecting different CNT architectures demonstrates a versatile strategy for frequency-selective absorption—a feature lacking in most conventional absorbers, which typically require reformulation rather than structural variation.

In summary, these findings highlight that core–shell structures and surface engineering provide a versatile platform to address the often conflicting requirements of high electromagnetic loss and good impedance matching. By judiciously selecting the core composition, shell material, and interfacial architecture, one can independently tailor the dielectric and magnetic properties, enhance corrosion resistance, and even achieve frequency-selective absorption. For absorbing materials used in integrated circuit packaging, which often need to operate reliably under harsh environmental conditions while maintaining an ultra-thin profile, such multifunctional core–shell designs offer new design insights toward durable, high-performance, and process-compatible absorbing solutions.

4.3. Three-dimensional Porous/Network Structure

In the design of wave-absorbing materials for integrated circuits, the three-dimensional porous/network structure strategy adeptly balances three core and interrelated requirements: ultra-thin thickness, lightweight, and good thermal conductivity. Achieving ultra-thin thickness and lightweight primarily relies on ingenious structural design. Zhang *et al*. [77] utilized a ZnMo-HZIF precursor to achieve in-situ foaming during mechanical ball milling, forming a three-dimensional foam structure rich in bubbles and pores. This not only significantly reduced the material density but also optimized its impedance matching characteristics, making it easier for electromagnetic waves to enter and be effectively attenuated within the material. With a low filler loading of only 15 wt.%, this material achieved a minimum reflection loss of −47.56 dB and an effective absorption bandwidth of 4.40 GHz at a thickness of 2.5 mm, almost covering the entire X-band. The in-situ foaming process forms a hierarchical porous foam with bubble-like cavities. These pores play a dual role: on one hand, they introduce air gaps that reduce the effective permittivity, optimizing impedance matching; on the other hand, the curved pore walls act as scattering centers, inducing multiple internal reflections that extend the propagation path of electromagnetic waves. The highly conductive MoC phase provides conduction loss along the pore walls. The synergistic effect of porosity and the conductive network enables the foam to achieve strong absorption even at a low filler loading. Zhang *et al*.'s MoC foam achieves low filler loading and good X-band absorption performance. However, its thickness of 2.5 mm remains an order of magnitude larger than typical chip-to-substrate gaps, leaving substantial room for optimization. Moreover, the

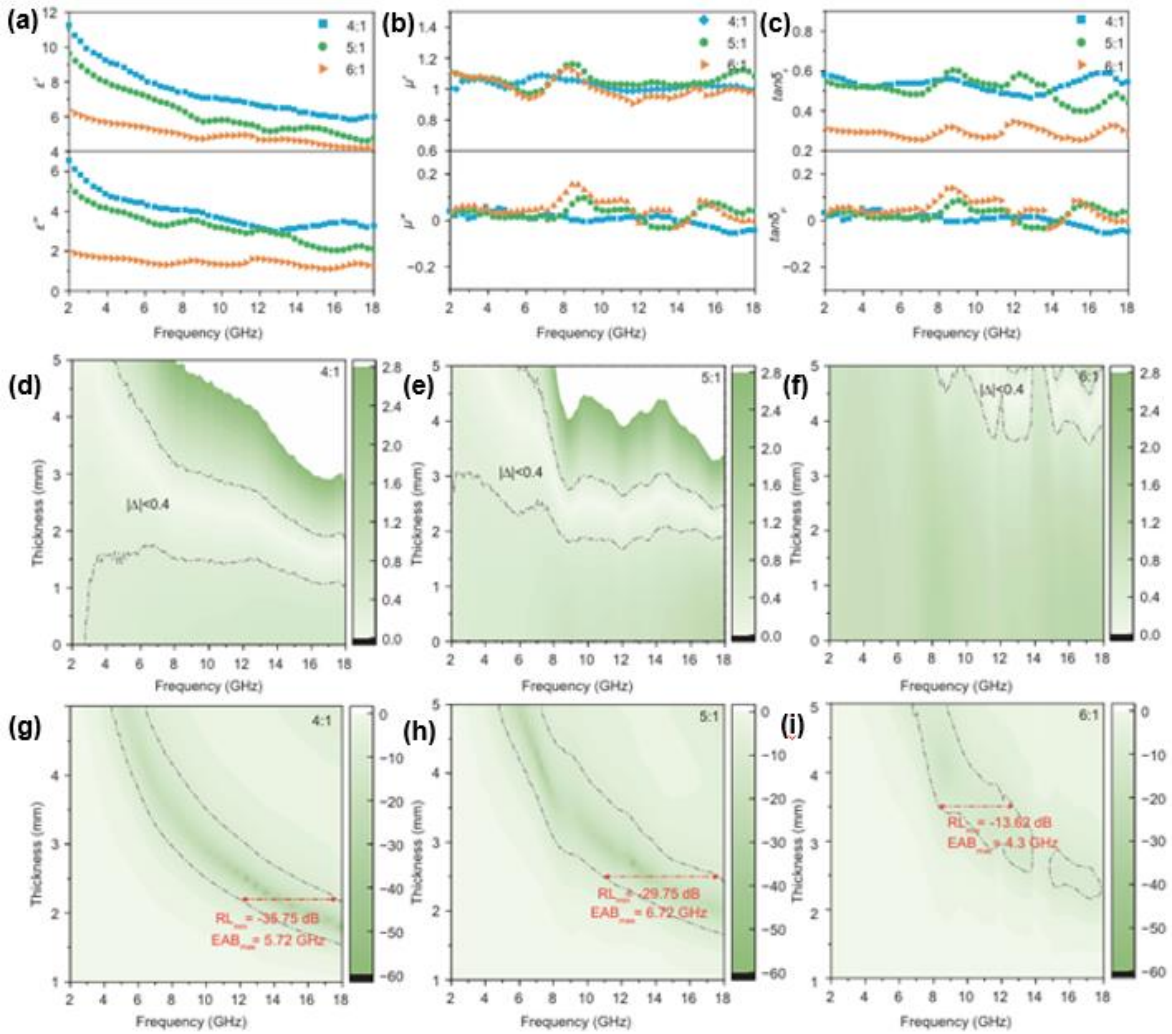

Figure 7: (a) ε' and ε'', (b) μ' and μ'', and (c) tan δ_ε and tan δ_μ of (Co@NCNTs)@BNNS/ScPEG composites. (d–f) Impedance matching of (Co@NCNTs)@BNNS/ScPEG composites. (g–i) RL_{min} and EAB_{max} of (Co@NCNTs)@BNNS/ScPEG composites. Reproduce with permission [78]. Copyright, 2025 Oxford academic.

in-situ foaming process involves high-temperature carbonization, exceeding the CMOS thermal budget, and the porous structure is mechanically fragile, risking collapse during underfill dispensing or thermal cycling.

Inspired by the hierarchical structure of a cactus, Qi *et al.* [78] designed and fabricated a cactus-like three-dimensional heterostructured network (Co@NCNTs)@BNNS/ScPEG composite absorbing material. By directional assembly, they constructed horizontal boron nitride nanosheet thermal conduction pathways and vertical cobalt-catalyzed nitrogen-doped carbon nanotube arrays, forming an integrated three-dimensional interconnected network that combines efficient thermal management with broadband microwave absorption. At a filler mass fraction of 30 wt%, a BNNS to Co^{2+} mass ratio of 5:1, and a matching thickness of 2.5 mm, the composite achieves a minimum reflection loss of –29.75 dB and an effective absorption bandwidth of 6.72 GHz, fully covering the Ku band (Fig. **7**).This work successfully addresses the challenge of synergistically improving thermal conductivity and wave absorption performance, providing a novel design concept and an effective approach for integrated thermal-electromagnetic management materials required by next-generation high-density electronic devices. The cactus-like network orthogonally integrates horizontal BNNS thermal conduction layers and vertical Co@NCNT absorbing arrays. The electrically insulating BNNS does not contribute to electromagnetic loss but provides a thermal conduction pathway, meeting the heat dissipation requirements of high-density packaging. The Co nanoparticles loaded on the vertical NCNTs introduce three loss mechanisms: conduction loss along the CNT walls, natural resonance magnetic loss from Co, and defect-induced dipole polarization from nitrogen doping. The hierarchical porous structure further promotes multiple reflections. This integration of function-specific microstructures for thermal conduction and microwave absorption embodies an advanced concept of co-design. The (Co@NCNTs)@BNNS/ScPEG composite uniquely integrates horizontal BNNS thermal conduction pathways with vertical carbon

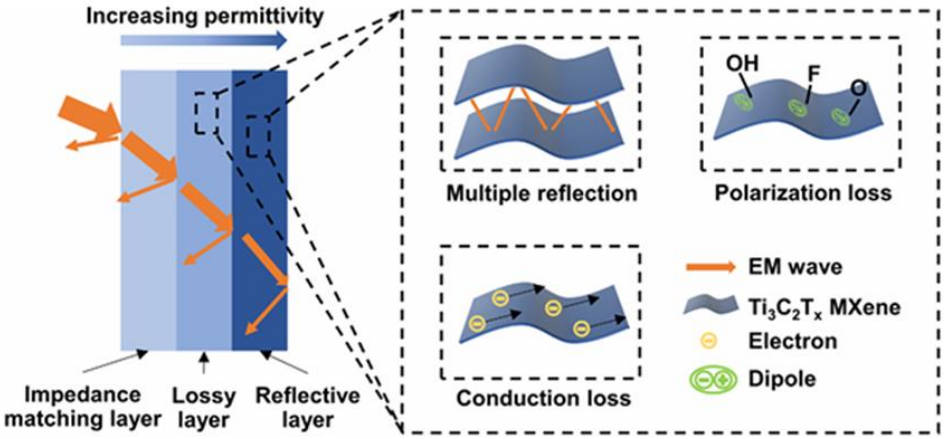

Figure 8: The electromagnetic absorption mechanism of the three-layer gradient structure. Reproduce with permission [79]. Copyright, 2022 Wiley-VCH Verlag GmbH.

nanotube arrays, achieving simultaneous microwave absorption and thermal management—a multifunctionality rarely seen in other porous designs. However, for integrated circuit packaging applications, critical limitations remain. For instance, the high filler loading increases the effective permittivity, potentially aggravating parasitic capacitance in dense interconnects. Moreover, the directional assembly process is low-throughput, and the hierarchical network is mechanically fragile, risking delamination during thermal cycling or underfill dispensing. Therefore, while this work provides a proof-of-concept for integrated thermal-electromagnetic management, practical deployment in advanced packaging requires substantial thickness reduction, lower filler content, and robust mechanical integrity validation.

4.4. Multilayer/Graded Structure

Besides the magnetic-dielectric composite approach for achieving broadband absorption, adopting a multilayer/gradient structure design is also an excellent strategy. This method can simultaneously reduce the thickness of wave-absorbing materials, enabling an ultra-thin profile. Zhang *et al*. [79] designed a $Ti_3C_2T_x$MXene/PVA three-layer gradient composite film. Its top layer has a low MXene concentration, forming a low-permittivity layer that ensures good impedance matching with air and allows electromagnetic waves to enter the material interior as much as possible. The middle layer adopts a moderate concentration, serving as a transition zone for preliminary attenuation. The bottom layer features a high MXene concentration, constituting a high-permittivity layer responsible for strongly dissipating the electromagnetic waves that have entered (Fig. **8**). By optimizing the structural parameters, this gradient material achieved full coverage of the effective absorption bandwidth across the X-band, along with an excellent minimum reflection loss of –74.8 dB. The three-layer gradient design exploits permittivity to modulate impedance matching: the top layer (low MXene concentration) possesses a low ε′, serving as an impedance transformer to minimize reflection; the middle layer (moderate concentration) provides transitional attenuation; the bottom layer (high concentration) exhibits a high ε′, achieving strong dissipation through conduction loss and interfacial polarization. The gradient change in MXene concentration creates a smooth transition of ε′ along the wave propagation direction, avoiding abrupt impedance discontinuities. This design mimics a quarter-wavelength transformer, but each layer satisfies the λ/4 condition at different frequencies, resulting in overlapping absorption peaks and thus broadband effective absorption. This three-layer gradient MXene/PVA film achieves high absorption across the entire X-band, outperforming most homogeneous absorbers of comparable thickness. Its graded permittivity design—low at the top for impedance matching and high at the bottom for strong dissipation—elegantly resolves the trade-off between wave entry and energy loss. However, several limitations arise for integrated circuit packaging. First, the layer-by-layer casting process is difficult to scale for wafer-level deposition and may introduce interfacial defects or delamination under thermal stress due to mismatched thermal expansion between layers. Second, the use of PVA as a matrix raises reliability concerns under high-humidity and reflow conditions, as PVA is hygroscopic and softens above 80 °C. In summary, while this gradient approach is highly effective for macro-scale absorbers, its translation to chip-level electromagnetic protection requires thinner construction and CMOS-compatible processing.

4.5. Solution Method and Coating Technology

Solution-based and coating techniques refer to material preparation methods in which materials are formulated into solutions, slurries, or sol states, applied

onto a substrate via specific means, and subsequently formed into functional thin films or coatings after processes like drying and curing. These techniques have become one of the mainstream methods for synthesizing ultra-thin wave-absorbing materials, owing to their capability to produce ultra-thin, uniform films and their ease of integration with integrated circuit fabrication processes. In practice, solution-based and coating techniques encompass various specific processes. Spin coating relies on the high-speed rotation of a substrate, using centrifugal force to spread the solution uniformly into a thin film. It is particularly suitable for preparing uniform films ranging from nanometers to micrometers in thickness on flat, small-area substrates, although material waste can be relatively high. Dip coating involves immersing a substrate into a solution and then withdrawing it to form a liquid film. This method is simple and can coat complex shapes, but the drying stage is susceptible to environmental interference. Slot-die coating applies the solution onto a moving substrate through a precision-controlled slot die head. It offers low solution waste and easy scalability to roll-to-roll mass production, but its process parameter optimization is complex. Spray coating atomizes the solution using an air stream and then sprays it onto the substrate, enabling rapid processing of large and curved surfaces, but it can be challenging to control film uniformity and thickness precisely. The sol-gel coating process typically uses precursors like metal alkoxides, which undergo hydrolysis and condensation to form a sol. This sol is then applied via methods like spin or dip coating. Subsequent gelation and heat treatment yield the final coating. This technique allows for precise control of coating composition, produces uniform films, and often requires lower processing temperatures.

Many researchers have utilized solution-based and coating techniques to fabricate numerous thin-film wave-absorbing materials with excellent performance. Addressing the preparation of flexible ultra-broadband absorbing films, Niu *et al.* [70] employed a liquid–liquid phase separation strategy to prepare PNIPAM/ionic liquid gel films on flexible substrates via spin coating. The film forms abundant conductive nanochannels and heterogeneous interfaces internally, achieving an ultra-wide effective absorption bandwidth of up to 34.96 GHz, along with excellent flexibility and transparency. Spray coating and atomized deposition represent another key technique. Their advantages include good coverage, high production efficiency, ease of applying functional coatings on complex package structure surfaces, and suitability for complex-shaped and non-planar integrated surfaces. The core steps are atomization, transport, and deposition: the solution or slurry is transformed into micron-sized droplets via a spray gun or ultrasonic atomizer; these droplets are carried by a carrier gas toward the substrate; upon impacting the substrate, the droplets spread, coalesce, and the solvent evaporates, forming a coating. The liquid–liquid phase separation strategy creates a bicontinuous network of conductive nanochannels within a flexible PNIPAM gel, achieving an exceptionally broad effective absorption bandwidth of 5–40 GHz—the widest reported for a single-layer absorber—while the gel exhibits remarkable mechanical toughness and repairability. On the downside, the material relies on ionic liquid (IL) for conduction loss; IL leakage remains a general concern for long-term reliability. Thermogravimetric analysis shows a 2 wt% mass loss already at 100 °C, indicating limited thermal stability above this temperature. Xie *et al.* [80] coated a mixed slurry of liquid-metal-encapsulated carbonyl iron/nickel (Fe/Ni@LM) microspheres and polydimethylsiloxane onto a flexible substrate, successfully preparing a high-performance wave-absorbing coating. This coating achieved an ultra-wide effective absorption bandwidth of 9.05 GHz at an ultra-thin thickness. The core–shell Fe/Ni@LM microspheres, when composited with PDMS, achieve an ultra-broadband effective absorption bandwidth of 9.05 GHz, covering the entire Ku band and most of the X band, with a minimum reflection loss of −54.73 dB. However, several practical drawbacks are significant. First, the optimal absorber requires a high filler loading of 70 wt% and a matching thickness of 2.43 mm, which is far thicker than typical packaging gaps. Second, the fabrication involves manual grinding of liquid metal with metal powders, making it difficult to control uniformity in large-scale production. Finally, the liquid metal shell may undergo oxidation over time, potentially altering the dielectric performance.

Table 1: Comparison of Specific Parameters of Various Wave-absorbing Materials

Design Strategy	Material System	RL (dB)	EAB (GHz)	Thickness (mm)
Magnetic-dielectric synergistic	$(CoCrFeCuNi)_3O_4$@C-graphene/PLA	-60.9	4.9	1.6-2.0
Core-shell (triple-layer)	FeCo@SiO_2@PANI	-69.5	8.6	2.9
Core-shell (ceramic)	DG/Si_3N_4	-77.3	7.44	-
3D porous foam	MoC foam	-47.56	4.40	2.5
Multilayer/gradient	$Ti_3C_2T_x$ MXene/PVA	-74.8	FullX-band	-

Furthermore, how to regulate impedance matching and the conductive network is a critical challenge in solution-based coating techniques for fabricating wave-absorbing materials. Luu *et al.* [81] employed solution dispersion and chemical coating techniques to successfully prepare lightweight Fe_3O_4/rGO@SiO_2 nanocomposite absorbing materials. Through liquid-phase homogeneous mixing and in-situ coating, they achieved stable modification and interfacial regulation of SiO_2 on Fe_3O_4/rGO. The chemically coated sample achieved a minimum reflection loss of –60.11 dB and an effective absorption bandwidth of 10.65 GHz at a filler loading of only 15 wt% and a matching thickness of 1.7 mm, while the mechanically milled sample (FRS1) achieved –54.18 dB and a bandwidth of 11.05 GHz at a thickness of 1.5 mm (Fig. **9**). Nevertheless, this work reveals several material-level shortcomings. For example, the amorphous SiO_2 shell may introduce additional mass without contributing to magnetic loss. Furthermore, the long-term stability of the composite under humid or thermal cycling conditions has not been assessed; if the shell is not sufficiently dense, the SiO_2-coated magnetic nanoparticles may still undergo oxidation. In addition, Bobsin *et al.* [69] developed an environmentally friendly aqueous graphene suspension using carboxymethyl cellulose as a dispersant, and employed spray coating technology to fabricate ultra-thin electromagnetic shielding/absorbing films on the surface of SiP (system-in-package) modules. This solution-based process is green, non-toxic, and suitable for large-area conformal coating. After annealing at 300 °C, the film exhibits a low resistivity of 2.8×10^{-2} Ω·cm and achieves an electromagnetic shielding effectiveness of –9 dB at 1 GHz (Fig. **10**). The water-based graphene suspension using carboxymethyl cellulose (CMC) as a dispersant offers an environmentally friendly, low-cost route to form conductive coatings on SiP modules via spray coating. However, this approach still exhibits several limitations. First, the shielding effectiveness is primarily reflection-dominant, and the value of −9 dB is modest compared to metallic shields. Second, the small lateral size of the graphene flakes increases the number of flake-to-flake junctions, degrading electrical conductivity. Finally, due to the high contact angle of the water-based ink, achieving uniform coating on complex three-dimensional SiP surfaces remains challenging.

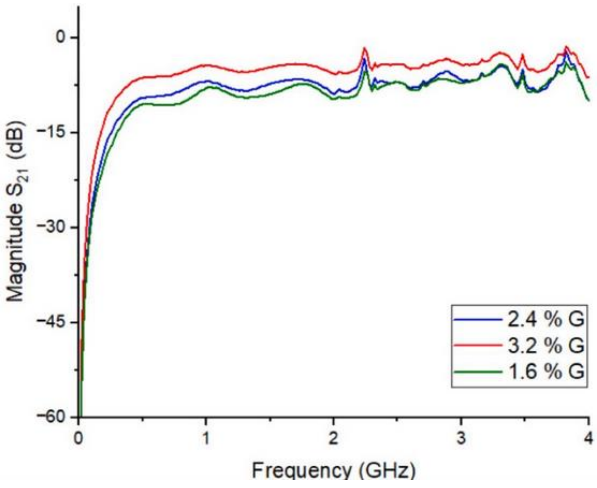

Figure 10: Shielding effectiveness (S 21) in frequencies between 30 MHz and 4.0 GHz [69]. Copyright, 2024 Elsevier.

However, solution-based coating techniques face several increasingly critical challenges when

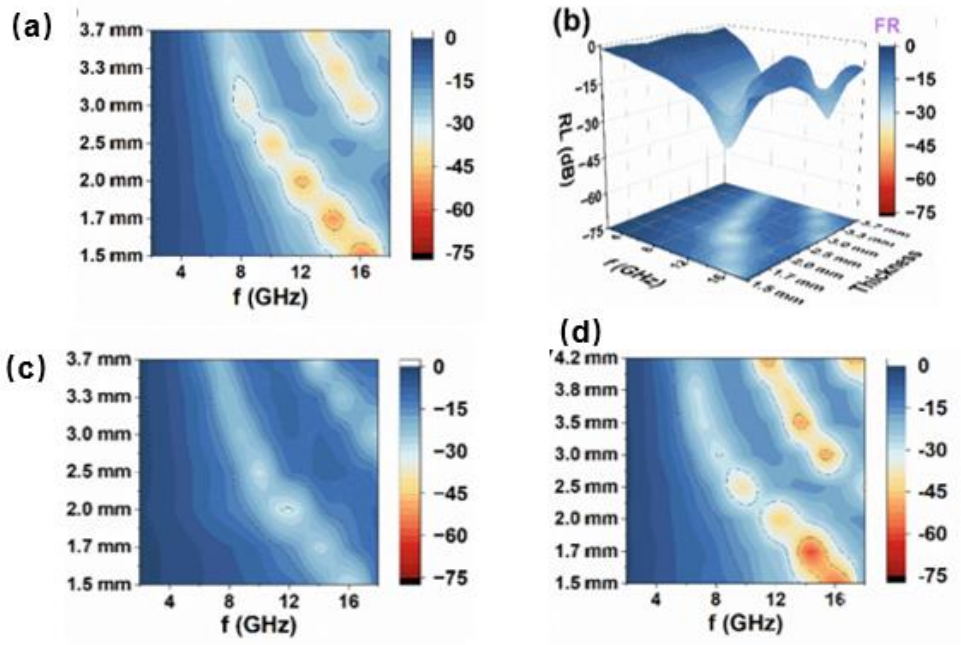

Figure 9: (a) Simulated three-dimensional RL pattern of FR, (b) projection of FRS1, (c) projection of FR, (d) projection of FRS2 [81]. Copyright, 2026 Elsevier.

transitioning from laboratory-scale preparation to industrial-scale manufacturing. Process reproducibility is influenced by multiple interdependent parameters: for example, the long-term stability of nanofiller dispersions is affected by agglomeration or sedimentation over time; batch-to-batch variations in precursor concentration and viscosity, environmental factors (temperature, humidity), and substrate surface conditions all impact process reproducibility. Even minor fluctuations can lead to significant deviations in the final film thickness, sheet resistance, and electromagnetic performance. For instance, the water-based graphene suspension developed by Bobsin *et al*. required precise control of carboxymethyl cellulose concentration and centrifugation steps to achieve consistent resistivity; deviations resulted in increased microvoids and agglomerates [69].

The uniformity of large-area coating remains a formidable challenge. Spin coating, while excellent for small, flat wafers, suffers from radial thickness non-uniformity and wastes a substantial amount of material. Slot-die coating offers better scalability but requires precise control of ink rheology, web speed, and gap distance. Spray coating can cover complex three-dimensional surfaces, but droplet size distribution, impact dynamics, and solvent evaporation rate all affect the film morphology. Achieving a thickness tolerance of ±5% across a 300 mm wafer or panel is challenging [82].

Defects in large-scale fabrication include pinholes, cracks, delamination, and particulate contamination. Pinholes arise from trapped air bubbles, insufficient wetting, or dust particles, and may create localized conductive paths that short-circuit the absorber to the underlying metallization layer. Cracking occurs when drying stresses exceed the cohesive strength of the film, especially for thick coatings or those with high filler loadings [83, 84]. Delamination between multilayer films or between the absorber and the package substrate results from thermal expansion mismatch or poor adhesion. These defects not only reduce absorption efficiency but also pose long-term reliability risks under thermal cycling and humidity exposure [85].

To mitigate these issues, several strategies are currently being explored. First, the addition of surfactants, dispersants, or binders (e.g., CMC, PVP) can improve colloidal stability and film-forming properties. Second, slow, staged drying or the use of solvent mixtures can help reduce the coffee-ring effect and cracking [86]. Third, optimizing filtration and degassing procedures removes particulates and air bubbles. The transition from laboratory-scale validation to large-scale industrial production remains an open challenge, requiring close collaboration among researchers, coating equipment suppliers, and semiconductor fabs.

4.6. Template method

The core of the template method lies in utilizing a material with a specific spatial structure as a "mold." By filling, transforming, or coating this mold and subsequently removing it, the negative or complementary structure of the mold is replicated. This method can be combined with synthesis processes such as embedding-sintering and template-etching and is applicable to various wave-absorbing material systems, including carbon materials and ceramics. This flexibility is beneficial for constructing materials with specific structures and optimizing their performance. The method is primarily divided into hard-template and soft-template approaches. Hard-template methods include salt templates, metal-organic framework (MOF) templates, melamine foam templates, etc., while soft-template methods include surfactant templates, among others. Among these, hard-template methods are more commonly used in the development of wave-absorbing materials for integrated circuits (ICs) due to their strong structural controllability and ease of scale-up production. The fundamental preparation principle involves using the spatial confinement effect of the template to directionally load carbon sources, magnetic components, or dielectric components into the pores or onto the surface of the template. After post-treatments such as carbonization or pyrolysis, the template is removed, yielding wave-absorbing materials with specific structures like hollow cavities, three-dimensional porous frameworks, or core-shell configurations. The unique structures constructed via this method can increase the material's specific surface area, establish continuous conductive networks, and introduce multiple heterogeneous interfaces, thereby enhancing the synergistic effect between dielectric loss and magnetic loss. Simultaneously, it significantly reduces the material's filler loading, avoiding interference with the electrical performance of IC devices. Currently, mainstream hard-template applications include: the salt template method, which leverages low cost and easy removal to prepare hollow carbon-based wave-absorbing materials; the MOF template method, which utilizes its compositional tunability to precisely prepare metal-nitrogen-doped carbon (M-N-C) single-atom or magnetic composite wave-absorbing materials; and the melamine foam template method, used to construct three-dimensional network-structured, high-temperature-resistant wave-absorbing materials. Wave-absorbing materials prepared by these template methods exhibit excellent performance in high-frequency bands [87-89].

To address the challenge of in-situ construction of hierarchical heterostructures using preforms or fiber templates, Fang *et al.* [90] employed a powder bed fusion (PBF) combined with chemical vapor reaction (CVR) template method. Using carbon fibers as the growth substrate, they in-situ grew β-SiC nanowires within a porous SiC ceramic preform. As the C_f content increased from 0 wt% to 15 wt%, the growth amount of SiC nanowires increased significantly, and the maximum dielectric loss tangent of the material rose from 0.8 to 1.6 (Fig. **11**(d)). At a C_f content of 15 wt% and a matching thickness of 2.1 mm, the sample achieved a minimum reflection loss of –40.2 dB and an effective absorption bandwidth of 3.28 GHz (9.45–12.73 GHz), mainly covering the X-band (Fig. **11** (a)–(c)). However, this approach exhibits several inherent limitations. First, the two-step process involves high temperatures and long durations, making it energy-intensive and incompatible with temperature-sensitive substrates. Second, the matching thickness of 2.1 mm remains relatively large, and the effective absorption bandwidth (3.28 GHz) is modest compared to many carbon-based absorbers. Third, the carbon fibers and residual amorphous carbon after CVR may introduce undesirable variations in electrical conductivity, affecting reproducibility. Furthermore, Liu *et al.* [91] used SiC fibers as one-dimensional templates and, through a Pd-free electroless nickel plating process activated by MXene self-reduction of Ag nanoparticles, constructed hierarchical heterostructured SiC@MXene/Ag@Ni (SMN) wave-absorbing fibers. This template method enabled directional loading of heterogeneous components onto the fiber skeleton, forming a continuous conductive network and multiscale interfaces. After 60 min of plating, the optimal performance was achieved: a minimum reflection loss of –45.84 dB and an effective absorption bandwidth of 4.54 GHz at a matching thickness of only 1.4 mm (Fig. **12**(a),(b)). The attenuation constant increased to 353.2, confirming that the template-directed structure significantly enhances electromagnetic wave attenuation capability (Fig **12**(c)). CST simulations showed a maximum radar cross-section (RCS) reduction of 29.86 dB·m² (Fig. **12**(d)). However, this work also reveals several shortcomings. The electroless plating process requires precise control of pH, temperature, and time, and over-plating leads to Ni agglomeration and degraded performance. Second, during the self-reduction step, MXene sheets inevitably undergo partial oxidation, which reduces electrical conductivity and may compromise long-term stability.

To precisely tune porosity via a hard template method for optimizing wave absorption performance, Liu *et al.* [92] used phenolic resin as the carbon source and nano-zinc oxide as a hard template. By adjusting the mass ratio of template to carbon source, they successfully synthesized layered hard carbon microwave-absorbing materials with hierarchical porous structures. A homogeneous paste-like precursor was first prepared by thoroughly mixing a solution of

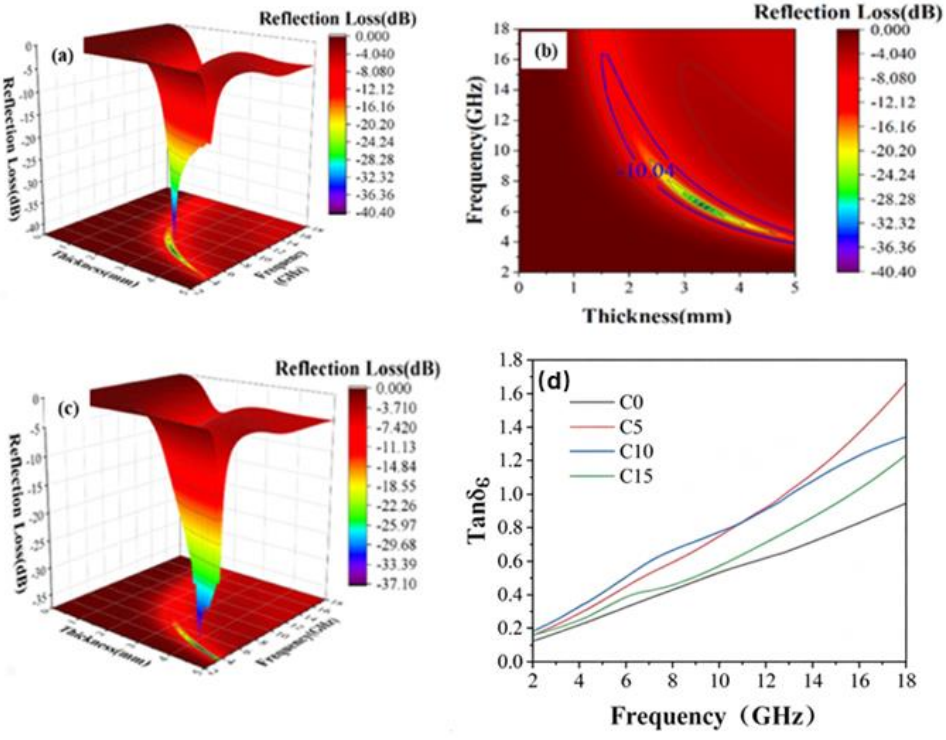

Figure 11: The reflection loss of C f /SiC wave absorbing materials at 2~18 GHz: (a) (b): C0; (c): C5(d)Dielectric property of Cf/SiC wave absorbing materials: Dielectric loss angle [90]. Copyright, 2025 Elsevier.

phenolic resin, ethanol, and water with ZnO nanoparticles. This precursor was carbonized at 700 °C under a nitrogen atmosphere to yield a ZnO/C composite. Subsequently, through vacuum annealing at 1250 °C, a carbothermal reduction reaction occurred, reducing ZnO to gaseous zinc, which—along with carbon monoxide—was removed, thereby leaving numerous nanoscale pores within the layered hard carbon structure. By varying the ZnO content in the precursor, a series of porous hard carbon samples with specific surface areas progressively increasing from 1 m²/g to 799 m²/g were successfully fabricated. Notably, the sample with a filler loading of 16.7 wt% exhibited a minimum reflection loss of –45 dB at a thickness of 2.0 mm, along with an effective absorption bandwidth of 4.08 GHz. In summary, the template method, by pre-constructing templates with specific spatial configurations, enables precise replication or induced formation of the target microstructure of wave-absorbing materials. This allows the realization of structural features such as hierarchical porosity, core–shell architectures, and heterointerfaces, which are beneficial for multiple reflections and interfacial polarization of electromagnetic waves. Nevertheless, several obvious drawbacks remain. The synthesis requires two annealing steps: first carbonization at 700 °C, followed by reduction-evaporation of ZnO at 1250 °C—the latter is extremely energy-intensive and difficult to scale up for mass production. Moreover, according to TG-DTA analysis, approximately 6 wt% of residual ZnO remains in the final product, which may cause undesirable catalytic effects or alter long-term stability. For integrated circuit packaging applications, the template method achieves low filler loading and light weight of absorbing materials while simultaneously optimizing impedance matching through the regulation of porosity and interfacial properties. This provides an important route for developing high-performance absorbing materials compatible with advanced packaging processes.

While the template method offers advantages in constructing wave-absorbing materials with unique structures, it simultaneously faces challenges related to template selection and structural control. Finding a template that is structurally ideal, chemically compatible, easy to remove, and cost-effective is no simple task. Some hard templates introduced to create specific porous structures must typically be removed after fulfilling their pore-forming role through methods such as strong acid or alkali etching or high-temperature calcination. This step not only increases process complexity and time costs, but the harsh chemical or thermal treatment conditions may also damage the structural integrity of the final product or even alter its electromagnetic properties, causing performance to deviate from expectations [93-95]. Furthermore, the essence of the template method lies in controlling material structure by replicating the template's morphology. However, this control is often at the

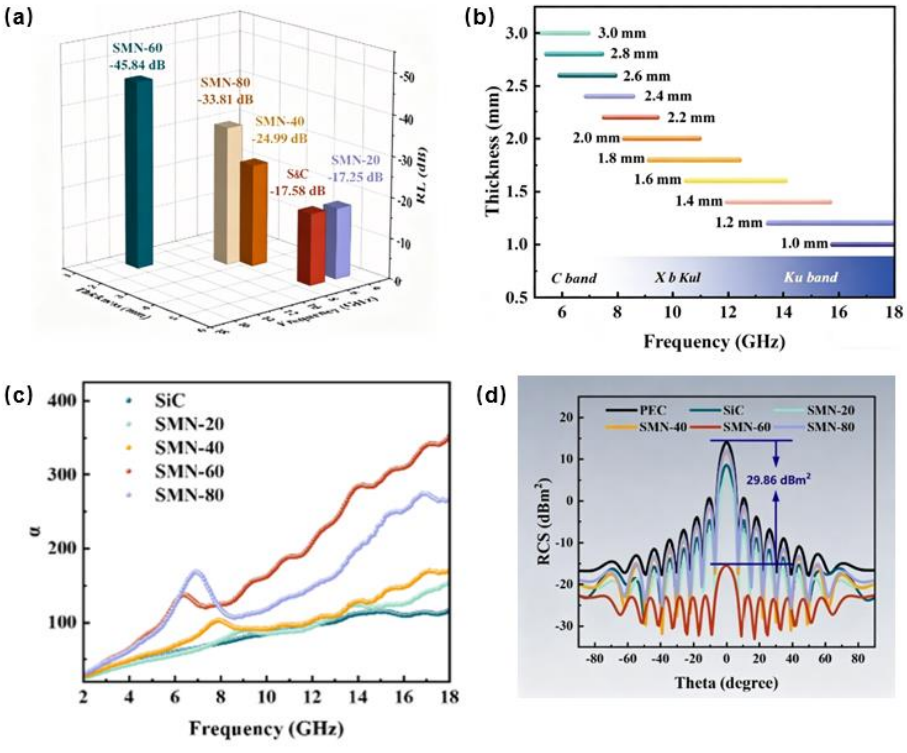

Figure 12: (a) 3D bar chart of RL min for SiC, SMN-20, SMN-40, SMN-60, and SMN-80,(b) EAB of SMN-60 at different thicknesses,(c) Attenuation coefficient of SiC and SMN samples,(d) the RCS simulation results at 13.56 GHz [91]. Copyright, 2026 Elsevier.

macroscopic or mesoscopic level. When precise control over details such as wall thickness, pore size distribution, or nanoscale features of heterogeneous interfaces is required, traditional template methods often prove inadequate. For instance, when constructing core-shell or hollow structures, performance metrics like effective absorption bandwidth depend heavily on the thickness and uniformity of the shell layer. Achieving a uniformly coated or completely filled shell with nanometer-level precision using template methods can be very difficult, potentially leading to defects or non-uniform thickness in the shell layer, which in turn affects the overall performance [96].

4.7. Additive Manufacturing

The application of additive manufacturing technology to the fabrication of electromagnetic wave-absorbing materials represents a highly promising direction in this field. It addresses many stringent requirements for wave-absorbing materials posed by integrated circuits. Complex structures such as three-dimensional porous, gradient, spiral, or lattice configurations, which are difficult to achieve with conventional processes, can be readily realized through 3D printing. These structures effectively extend the propagation path of electromagnetic waves, significantly enhancing energy dissipation through multiple reflections and scattering. When fabricating electromagnetic protection layers for chips via additive manufacturing, it is possible to directly print wave-absorbing materials onto specific areas of the chip, antenna, or package substrate—or even embed them within the package—to form integrated structural-functional components. This approach holds the potential to resolve issues associated with traditional patch-type wave-absorbing materials, such as interfacial thermal stress, poor adhesion, and the occupation of additional space, thereby enhancing both integration density and reliability.

In terms of utilizing additive manufacturing technology to construct bioinspired and gradient structures for broadband and wide-angle absorption, Deng *et al*. [97] successfully fabricated a biomimetic stepped structure composed of MWCNTs/NiFe/PETG composite material, featuring ultra-broadband and wide-angle wave absorption performance, by integrating additive manufacturing, machine learning, and bio-inspired structural design (Fig. **13**). The researchers utilized additive manufacturing technology to achieve complex three-dimensional periodic structures that are difficult to process with conventional methods. Furthermore, they deeply integrated material design and structural design in three-dimensional space, enabling active control over the propagation and attenuation of electromagnetic waves at the macroscopic scale. Experimental tests showed that this 3D-printed bio-inspired structure achieved an effective absorption bandwidth of 31.4 GHz within an ultra-wide frequency range of 2–40 GHz and maintained excellent absorption performance even at incident angles up to 65°. However, the 3D printing process causes surface

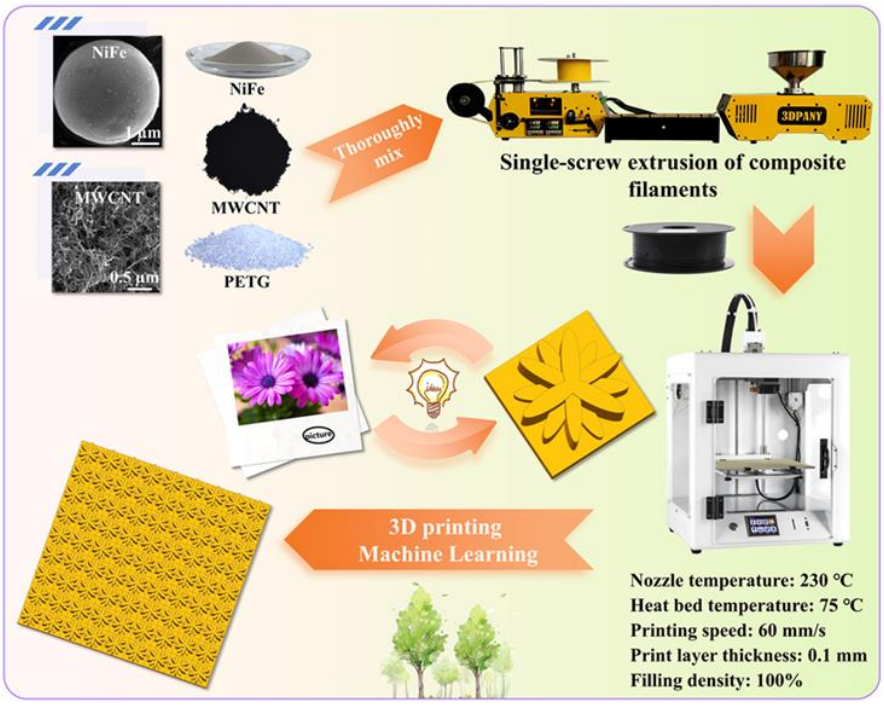

Figure 13: The preparation process of the superstructure of the bionic bone-point daisy. Reproduce with permission [97]. Copyright, 2025 Elsevier.

roughness and inhomogeneous filler distribution, resulting in a significant gap between the simulated effective absorption bandwidth (34.67 GHz) and the measured value (31.4 GHz). Second, the unit cell's base plate plus the three petal layers likely exceeds 8 mm in total thickness, making it incompatible with thin packaging. Moreover, the high NiFe loading (20 wt%) and 3 wt% MWCNTs increase density and cost, indicating that further optimization of the fabrication process and component ratios is still required. Furthermore, Yang *et al*. [98] successfully manufactured a wave absorber with a periodically arranged four-layer stepped structure using a graphene (GR)-FeSiAl/polylactic acid (PLA) composite as the raw material. The structure consists of a base plate with square holes at the bottom and three upper layers of cubes with gradient side lengths. This structural design achieves multi-scale loss mechanisms and good impedance matching (Fig. **14**). After optimizing the unit size, the stepped structure absorber reached a minimum reflection loss (RL min) of –36.01 dB and an effective absorption bandwidth of 12.75 GHz. Moreover, under both transverse electric (TE) and transverse magnetic (TM) polarizations, it maintained an effective absorption bandwidth exceeding 10 GHz across an incident angle range of 0° to 50°, demonstrating favorable wide-angle absorption characteristics. This 3D-printed design maintains an effective absorption bandwidth greater than 10 GHz at incident angles up to 50° under both TE and TM polarizations—a capability rarely achieved in simple coated plates. However, several shortcomings exist. Due to surface texture induced by 3D printing, angular misalignment in arch testing, and discrepancies between coaxial material characterization and full-structure measurements, the experimental effective absorption bandwidth is notably lower than the simulated value. Moreover, the high filler loading increases density and may cause agglomeration, while the PLA matrix limits the service temperature to below 60 °C.

To address the demand for broadband microwave absorption in high-temperature environments, Wang *et al*. [99] employed material extrusion 3D printing technology to design and integrally manufacture a SiC honeycomb metamaterial using silicon carbide ceramic as the base material. This 3D-printed SiC honeycomb structure exhibited excellent electromagnetic wave absorption performance at room temperature and an incident angle of 60°, with its effective absorption bandwidth covering 4.85 to 39.49 GHz, spanning 34.64 GHz. Furthermore, the structure demonstrated exceptional high-temperature stability. After undergoing in-situ exposure at 1000°C and erosion in an air atmosphere at 1600°C, it still maintained an effective absorption bandwidth exceeding 35 GHz at a 60° incident angle. Additionally, under oblique incidence conditions from 30° to 60°, for both TE and TM polarizations, the structure achieved broadband absorption over 30 GHz, showing excellent wide-angle adaptability. However, this approach still exhibits several drawbacks. The PIP process requires carbonization at 950 °C and involves multiple infiltration/pyrolysis cycles at temperatures up to 1200 °C, making the fabrication energy-intensive and time-consuming. Second, the resulting metastructure has an overall thickness of 18 mm and a density of 0.61 g/cm³—lightweight for a ceramic but still too heavy for chip integration. Yin *et al*. [100] designed a structure consisting of four helical pillars arranged periodically on a planar substrate. Using fused deposition modeling technology, they integrally fabricated this helical metamaterial via 3D printing with a carbon nanotube-doped acrylonitrile butadiene styrene composite. Through systematic optimization of structural parameters, this absorber demonstrated exceptional ultra-broadband absorption performance within the 2–40 GHz frequency range. Experimental measurements yielded an effective absorption bandwidth of 33.7 GHz, covering 3.5–5.1 GHz and 7.9–40 GHz, with a minimum reflection loss of –31.5 dB.

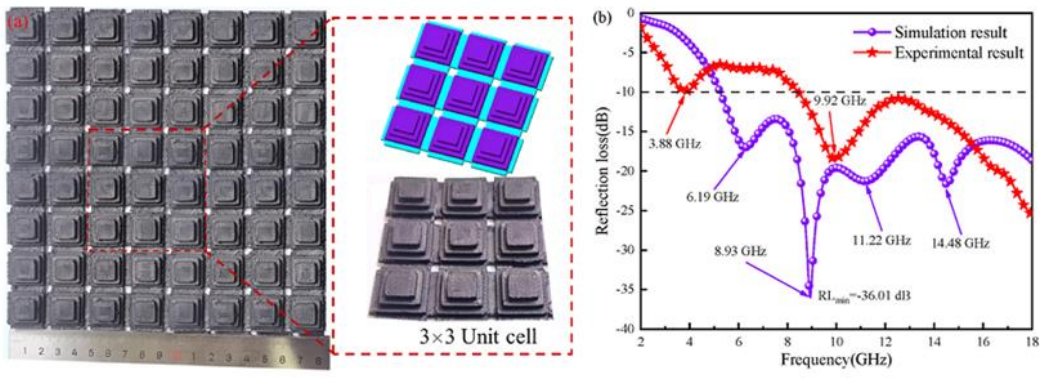

Figure 14: (a) Digital photos of the stepped structure, (b) Simulation and experimental reflectance curves of the stepped structure. Reproduce with permission [98]. Copyright, 2024 Elsevier.

In summary, additive manufacturing technology offers unprecedented freedom for the structural design of wave-absorbing materials. By precisely controlling three-dimensional periodic structures, gradient units, and bioinspired configurations, this technology can effectively extend the propagation path of electromagnetic waves, enhance multiple reflections and scattering, and thus achieve ultra-broadband, wide-angle stable absorption. For integrated circuit packaging, additive manufacturing is expected to overcome the limitations of traditional patch-type absorbing materials, such as interfacial thermal stress, poor adhesion, and additional space occupation, enabling in-situ, integrated incorporation of absorbing structures onto chips or packages. This provides a flexible and efficient solution for electromagnetic compatibility design in high-density, high-frequency integrated circuits.

However, additive manufacturing technology also faces several bottlenecks and limitations. Compared to the tens of thousands of material options available for traditional manufacturing, the variety of materials specifically designed for 3D printing—particularly those that simultaneously satisfy good printability and excellent wave-absorbing performance—is very limited. Additionally, the long-term stability of printed materials is often inferior to that of conventionally manufactured counterparts. On the other hand, when printing wave-absorbing materials via additive manufacturing, wave-absorbing fillers are typically incorporated into the feedstock. These fillers can severely interfere with the printing process. Moreover, additive manufacturing inherently suffers from certain process-related defects. The layer-by-layer deposition process can result in a stair-step effect on sloped or curved surfaces, adversely affecting surface finish. Such rough surfaces can scatter electromagnetic waves irregularly, disrupting the intended wave-absorption performance, especially at higher frequencies [101].

4.8. Application Schemes of Absorptive Materials in Integrated Circuits

The preceding sections have discussed the unique electromagnetic interference issues associated with various packaging technologies and, accordingly, proposed a series of design and synthesis strategies for wave-absorbing materials. The following will introduce specific applications of composite wave-absorbing materials in integrated circuits. Whether it is the crosstalk caused by high-density routing in redistribution layers (RDLs), the capacitive/inductive coupling between through-silicon via (TSV) arrays, or the self-interference and cavity resonance induced by mixed-signal integration in system-in-package (SiP), all pose severe challenges to package-level electromagnetic compatibility. However, traditional metal-based reflective shielding has inherent limitations in advanced packaging environments where space is constrained and multiple reflections are severe—reflected waves can easily excite cavity resonance, leading to secondary contamination. Therefore, the application of wave-absorbing materials offers distinct advantages.

For example, to address electromagnetic radiation interference in high-frequency chip packages, Huo *et al.* [102] proposed a novel ITO resistive-film metamaterial absorber for electromagnetic radiation suppression in system-in-package (SiP). The absorber uses glass as the substrate, with a top layer composed of a composite resistive film structure of crosses, rings, and L-shaped elements, and a bottom full-metal ground layer, forming a low-profile sandwich structure. Simulation results show that the absorber achieves an absorption rate above 90% in the 21–55 GHz frequency range (Fig. **15**(a)), exhibits polarization insensitivity and stable performance at large incidence angles, and equivalent impedance analysis confirms good impedance matching with free space within the operating band. When applied between the chip package heat spreader and the PCB, the radiated electric field at a distance of 3 m is suppressed by an average of 12.4 dB over 18–47 GHz, with a maximum suppression of 18 dB (Fig. **15**(b)). The measured results agree well with simulations, demonstrating effective mitigation of cavity radiation leakage in high-frequency packages. Regarding radiation suppression for high-frequency chip packages, Liu *et al.* [103] proposed a double-layer impedance-matching microwave absorbing structure. By inserting a lossless dielectric layer such as air between the metal backplane and the absorbing layer as a phase-control layer, the impedance mismatch problem of high-permittivity materials can be significantly improved. This structure was applied to and verified with three materials: graphene, $Ce_{0.75}Sm_{1.25}$ $Fe_{17}N_{3-\delta}$, and Mn. For the graphene composite system, with an air layer thickness of 1.9 mm and an absorbing layer thickness of 0.7 mm, the effective absorption bandwidth reaches 7.4 GHz (10.6–18 GHz) and the peak reflection loss is −31 dB. $Ce_{0.75}Sm_{1.25}$ $Fe_{17}N_{3-\delta}$, an ultra-thin absorbing layer of only 0.1 mm combined with a 2.8 mm air layer achieves strong absorption of −44 dB and an effective bandwidth of 8.5 GHz (9.5–18 GHz), with an areal density as low as 0.031 g/cm² (Fig. **16**(a)(b)). The Mn system improves from no effective absorption to a bandwidth of 6.9 GHz and a peak of −28 dB (Fig. **16**(c)(d)). Multiple-reflection modeling and Poynting vector analysis confirm that the air layer achieves impedance matching through phase-cancelation of reflected waves. Moreover, the air layer can be replaced by lossless

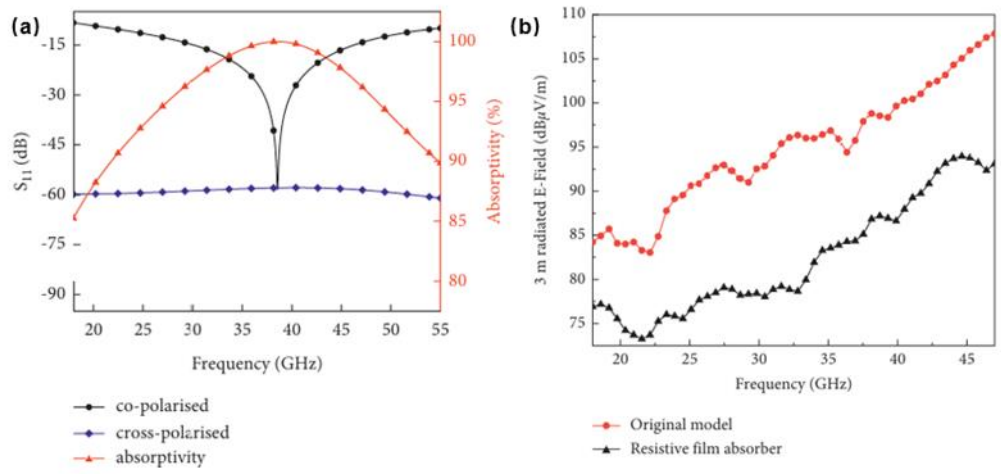

Figure 15: (a) Simulated copolarized and cross-polarized S11 (left column) and absorptivity (right column). (b) Radiated E-Field of package at 3m [102]. Copyright,2022 Wiley-VCH Verlag GmbH.

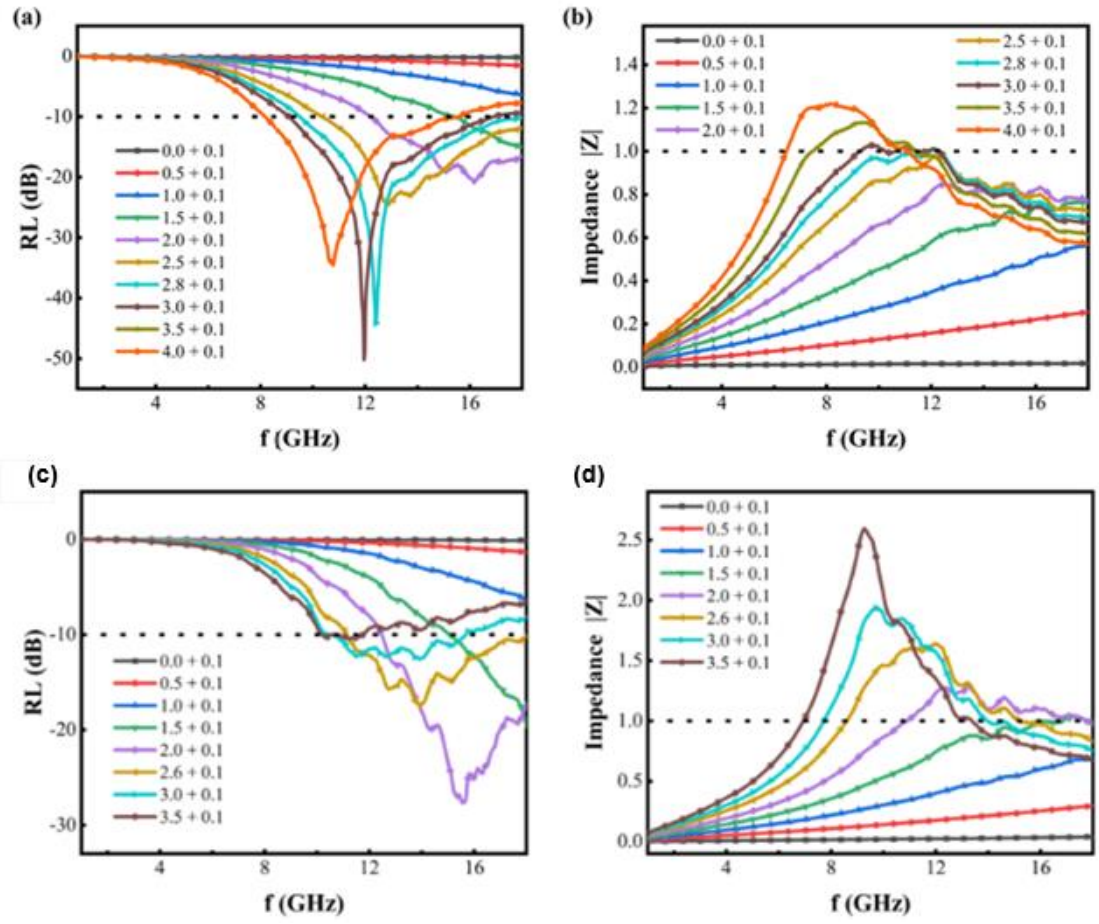

Figure 16: Frequency dependence of (a) RL values and (b) Impedance of the double-layer absorber composed of an air layer and a $Ce_{0.75}Sm_{1.25}Fe_{17}N_{3-\delta}$/Paraffin layer. Frequency dependence of (c) RL values and (d) Impedance of the double-layer absorber composed of an air layer and a Mn/Paraffin layer [103]. Copyright, 2022 Elsevier.

dielectrics such as paraffin or Teflon, offering the advantages of light weight, ultra-thin profile, and broadband performance. This provides a universal solution for enhancing the absorbing performance of high-loss but impedance-mismatched materials.

In addition to designing various structurally different absorbers, identifying multifunctional absorbing materials that combine high temperature resistance, excellent heat dissipation, and superior mechanical properties is also a key breakthrough point for solving electromagnetic interference issues in integrated circuits. For example, Li *et al.* [11] found that cobalt (Co), as a ferromagnetic metal, possesses both a high Curie temperature and thermal stability, and can provide both magnetic and dielectric losses, making it an ideal

absorbing material. Therefore, the researchers prepared cobalt particles with three morphologies—spherical, flower-like, and sword-like—using a liquid-phase reduction method, and systematically investigated their microstructure, magnetic properties, and wave-absorbing characteristics in the 2–18 GHz frequency range using SEM, XRD, VSM, and a vector network analyzer. The measurement results show that the sword-like cobalt particles achieve a reflection loss of −50.96 dB at a coating thickness of 1.6 mm and a frequency of 13.6 GHz, with an effective absorption bandwidth of 7.6 GHz. Their overall performance is significantly superior to that of the spherical and flower-like samples (Fig. **17**). A thin coating made of this cobalt-based absorbing material enables strong absorption and broadband coverage, aligning with the miniaturization and high-frequency trends of IC packaging. It can effectively suppress internal electromagnetic interference in packages, providing an efficient material solution for electromagnetic compatibility in advanced packaging.

In advanced packaging scenarios, the parasitic coupling and backside radiation of redistribution layers (RDLs) in wafer-level packaging (WLP), the through-silicon via (TSV) crosstalk and cavity resonance in 2.5D/3D packaging, and the self-interference from mixed digital/analog/RF integration in system-in-package (SiP) collectively constitute typical electromagnetic interference (EMI) challenges for integrated circuits. Traditional metal-based reflective shielding tends to cause secondary pollution and cavity resonance, making it difficult to meet the requirements for ultra-thin, lightweight, broadband, and highly reliable electromagnetic protection. In contrast, high-performance wave-absorbing materials based on composite structure designs such as magnetic-dielectric synergy, core-shell architectures, porous networks, and gradient multilayer configurations can achieve efficient electromagnetic wave dissipation through the synergistic action of dielectric loss, magnetic loss, interfacial polarization, and destructive interference. When combined with fabrication techniques including solution-based coating, template methods, and additive manufacturing, these materials can be integrated into advanced packaging processes such as WLP, 2.5D/3D packaging, and SiP in the form of thin films, coatings, or embedded structures.

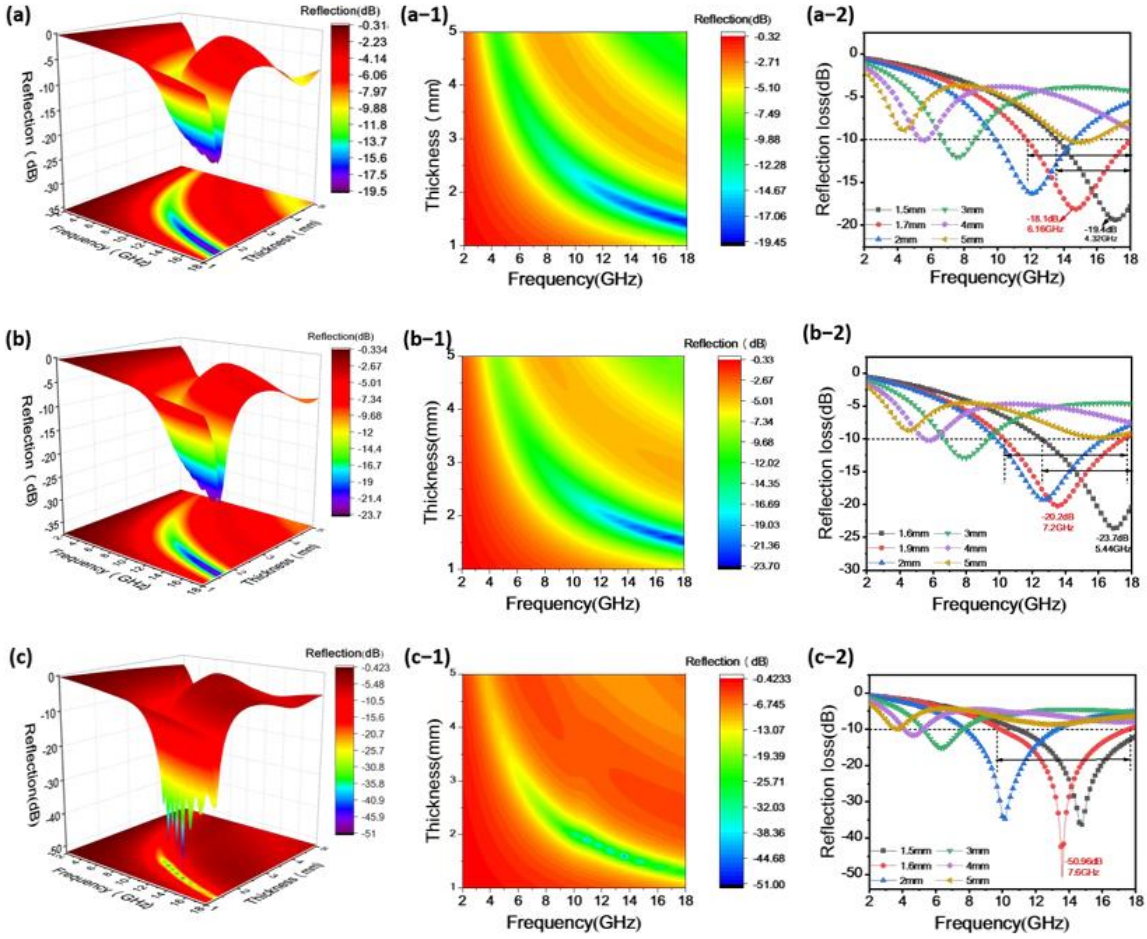

Figure 17: Three-dimensional (3D) RL, 3D projection plots, and the RL values of 70% Co content (a,a-1,a-2) spherical Co particles; (b,b-1,b-2) flower-like Co particles; and (c,c-1,c-2) sword-like Co particles [11]. Copyright,2023 Springer Science and Business Media LLC

Addressing the trends of 5G/6G millimeter-wave communication and high-density heterogeneous integration, multifunctional absorbing structures and in-situ integration schemes that combine broadband absorption, ultra-thin and lightweight characteristics, thermal dissipation, and high-temperature stability have become a key pathway to resolving package-level electromagnetic compatibility issues and supporting the stable operation of high-performance chips.

Although the aforementioned application schemes demonstrate the potential of wave-absorbing materials for electromagnetic interference suppression in advanced packaging, two critical issues must be addressed to bridge the gap between laboratory demonstrations and real-world IC manufacturing: CMOS process compatibility and industrial-scale integration.

From the perspective of CMOS compatibility, the thermal budget of back-end-of-line (BEOL) processes is typically limited to ≤450 °C to protect metallization layers and low-κ dielectrics. However, many high-performance absorbers require processing temperatures far exceeding this limit. For instance, the growth of SiC nanowires via CVD or CVR requires 600–1450 °C [74, 90]; hard carbon synthesis using a ZnO template demands annealing at 1250 °C [92]; and even spray-coated graphene films require annealing at 300 °C [69], which approaches the upper limit of BEOL compatibility. Consequently, the direct on-wafer integration of such absorbers is impractical unless alternative transfer or post-package attachment methods are employed. Contamination control is another stringent requirement: semiconductor fabs demand ultra-clean environments, yet many solution-based synthesis methods (sol-gel, hydrothermal, in-situ polymerization) involve toxic precursors, organic solvents, or ionic residues that are incompatible with cleanroom protocols. Residual carboxymethyl cellulose in aqueous graphene inks or unremoved ZnO templates can introduce mobile ions or particulate defects, compromising device yield and reliability [69, 92]. Moreover, the physical form of the absorber must withstand subsequent packaging steps such as solder reflow (260 °C), underfill dispensing, and thermal cycling. Rigid absorbers like ITO-on-glass cannot conform to curved package surfaces [102]; the 2.8 mm air gap in the double-layer design is impossible to maintain in a real package[103]; and fragile porous foams are prone to collapse during underfill injection [77, 78].

To address industrial-scale integration, issues of throughput, uniformity, cost, and reliability must be resolved. Solution-based coating techniques such as spin-coating, spray-coating, and slot-die coating are scalable and already used in semiconductor manufacturing, but achieving uniform dispersion of nanofillers over large areas remains difficult. Template methods can produce precise nanostructures, but the template removal steps (acid/alkali etching or high-temperature reduction) are difficult to integrate into mass production, resulting in low throughput and high cost. Additive manufacturing (3D printing) is inherently serial and slow; the millimeter-thick structures reported in are much slower than wafer-scale deposition methods, making them unsuitable for volume production except for niche applications or master mold fabrication [97-100]. Finally, the reliability of wave-absorbing materials is often overlooked; subsequent research should focus more on thermal cycling, humidity, and accelerated life testing.

Beyond CMOS compatibility and manufacturability, the practical deployment of wave-absorbing materials in IC packaging demands rigorous assessment of their long-term reliability, thermal stability, and mechanical durability under real device operating conditions. Thermal stability is a primary concern. Many high-performance absorbers rely on polymers, gels, or organic matrices that degrade at moderate temperatures. For example, the PNIPAM/ionic liquid gel exhibits a 2 wt% mass loss already at 100 °C, and its lower critical solution temperature (LCST) of ≈32 °C implies that the gel may undergo phase transitions and structural changes during normal device operation (which can reach 85–125 °C) [70]. Even the sword-like Co particles, though possessing a high Curie temperature, are prone to surface oxidation in air at elevated temperatures, which will gradually degrade their magnetic loss capability [11]. In contrast, the SiC honeycomb metastructure exhibits excellent high-temperature stability up to 1600 °C, but its fabrication process is energy-intensive and the material itself remains brittle [99].

Mechanical durability is equally important. Absorbers integrated into packages must withstand thermomechanical stresses arising from coefficient of thermal expansion (CTE) mismatches among the chip, substrate, mold compound, underfill, and the absorber itself. During thermal cycling, repeated expansion and contraction can lead to delamination, cracking, or interfacial failure. For instance, the three-layer gradient MXene/PVA film suffers from potential delamination due to interlayer CTE mismatch and the hygroscopic nature of PVA [79]. The fragile three-dimensional porous foams are likely to crumble during underfill dispensing or wire bonding [77, 78]. In contrast, the Fe/Ni@LM/PDMS coating offers flexibility, but its high filler loading (70 wt%) makes it stiff and prone to cracking upon bending [80].

Therefore, future efforts must prioritize the development of low-temperature dry processing routes, CMOS-compatible material systems, and robust reliability assessment. Only through such multi-directional co-design can wave-absorbing materials transition from academic breakthroughs to industrial solutions for next-generation IC packaging.

5. CONCLUSION

This paper systematically explores the design strategies and synthesis technologies of electromagnetic wave absorbing materials for integrated circuit applications. It analyzes the mechanistic characteristics of key design approaches, including magnetic-dielectric synergistic composites, core-shell structures and surface engineering, three-dimensional porous/network architectures, and multi-layer graded structures. Furthermore, it investigates the process characteristics and applicable scenarios of various synthesis methods, such as solution processing and coating techniques, templating methods, and additive manufacturing. Research indicates that through multi-component synergy and multi-scale structural innovation, significant progress has been achieved in broadband absorption, ultrathin thickness, lightweight integration, and compatibility with advanced packaging processes, providing crucial technical support for the electromagnetic protection of integrated circuits.

Among the various design strategies for wave-absorbing materials reviewed in this paper, three material systems show the greatest promise for integration into integrated circuit packaging. The first is solution-processed magnetic-dielectric nanocomposite coatings. Representative materials such as Fe_3O_4/rGO@SiO_2 and spray-coated graphene/CMC films combine a low processing temperature (≤300 °C), sub-millimeter thickness (1.5–1.7 mm), and good compatibility with existing spin-coating or spray-coating equipment in semiconductor fabs, demonstrating the best short-term application potential. These materials offer an effective absorption bandwidth of 10–11 GHz, a reflection loss of −54 to −60 dB, and a moderate filler loading (15 wt%) [69, 81]. Future optimization should focus on reducing the thickness to below 0.5 mm, completely removing residual dispersants, and verifying long-term stability under thermal cycling conditions.

The second is core-shell structures with multi-functional shells. Designs such as FeCo@SiO_2@PANI and hollow carbon/ZnO/LDH microspheres demonstrate that carefully engineered shells can simultaneously optimize impedance matching, suppress eddy currents, provide corrosion protection, and introduce additional polarization losses [73, 75]. However, the current matching thickness still needs to be significantly reduced. Future research should focus on developing ultra-thin shells and replacing expensive or toxic components with earth-abundant alternatives.

The third is 3D-printed metastructures for broadband, wide-angle absorption. Bio-inspired stepped, honeycomb, and helical metamaterials fabricated by additive manufacturing achieve ultra-broadband absorption of 31–35 GHz and angular stability up to 65°, which is unattainable with conventional planar coatings. Nevertheless, their millimeter-scale thickness (8–18 mm) and serial, low-throughput fabrication currently restrict them to macroscopic applications such as radar stealth and anechoic chambers [97-100]. For IC packaging, the same design principles can be miniaturized via high-resolution 3D printing (e.g., two-photon lithography) to embed sub-millimeter lattice absorbers into the redistribution layer or interposer.

However, despite these advancements, several challenges persist in the design and application of absorbing materials for integrated circuits, which still require further research and breakthroughs.Limitations in Design and Synthesis Strategies. Various design strategies face inherent challenges. Although magnetic-dielectric synergistic composites enable complementary loss mechanisms, achieving uniform dispersion and strong interfacial bonding between magnetic and dielectric fillers at the nanoscale remains difficult to precisely control, often leading to performance fluctuations. Core-shell structures and surface engineering can effectively modulate electrical conductivity and chemical stability; however, the nanoscale precision required for shell thickness control poses significant processing difficulties, and the controllable fabrication of multi-layer shell structures is highly complex. Three-dimensional porous/network architectures can simultaneously achieve lightweight properties and good thermal conductivity, but the trade-off between porosity and mechanical strength requires careful optimization—excessively high porosity can result in fragile structures that fail to meet packaging reliability requirements [68, 104, 105]. While multi-layer graded structure designs can broaden the absorption bandwidth, challenges related to interfacial bonding strength and thermal stress mismatch between layers are prominent, and achieving high precision and consistency in the fabrication of multi-layer structures is difficult. Future research should leverage multi-physics simulations and intelligent algorithms to optimize structural parameters, combined with advanced manufacturing techniques such as atomic layer deposition and nanoimprint lithography, to address these design deficiencies [106, 107].

The Compatibility between Synthesis Processes and Packaging Requirements Urgently Needs

Enhancement. Current mainstream synthesis methods exhibit process compatibility shortcomings when applied to integrated circuits. Although solution processing and coating techniques can produce ultrathin and uniform films, ensuring the long-term stability of nanofillers in solution remains difficult, and defect control—such as the formation of pinholes and cracks during film formation—is complex. Templating methods enable the construction of hierarchical pore structures, but the template removal process often involves strong acid/base etching or high-temperature treatment, which conflicts with the cleanliness requirements and thermal budgets of CMOS processes. Furthermore, precise control over nanoscale wall thickness and pore size distribution using templating methods remains limited. Additive manufacturing technologies offer the possibility of customizing complex structures; however, the range of printable absorbing material systems is restricted, the interference of high filler loadings during the printing process has not been effectively resolved, and surface roughness issues arising from layer-by-layer stacking can significantly degrade absorption performance at high frequencies [108, 109]. Future research needs to develop novel low-temperature, contamination-free synthesis processes compatible with advanced packaging flows, with a focus on achieving synergistic design of materials, processes, and packaging to enable in-situ integration and embedded fabrication of functional absorbing layers.

Beyond the immediate challenges, several emerging trends are poised to reshape the design, fabrication, and deployment of wave-absorbing materials for integrated circuits. Traditional trial-and-error approaches are time-consuming and often struggle to tune material compositions for optimal performance. In contrast, machine learning models, particularly deep neural networks, generative adversarial networks (GANs), and reinforcement learning, offer powerful tools for accelerating material discovery and property prediction. For example, ML can be trained on datasets of electromagnetic parameters to predict the optimal combination of filler morphology, shell thickness, and gradient architecture for targeted frequency bands. Inverse design algorithms can directly generate microstructures that satisfy desired impedance matching and loss criteria, as demonstrated by Deng *et al*., who used XGBoost and Bayesian optimization to optimize a 3D-printed stepped structure [97]. Future efforts should integrate multi-fidelity simulations to reduce computational costs. Moreover, explainable AI (XAI) could reveal hidden physical mechanisms, guiding rational design rather than blind optimization.

Next-generation ICs may require absorbers that can adapt to changing operating frequencies, power levels, or environmental conditions. Intelligent tunable absorbers can be realized through phase-change materials (e.g., VO_2, GST), whose dielectric properties switch reversibly under thermal, electrical, or optical stimuli. The integration of sensors and feedback control loops would enable real-time self-adjustment, maintaining optimal EMI suppression across dynamic scenarios. Although such concepts are still in early research stages for IC packaging, they hold promise for 6G communication systems, reconfigurable intelligent surfaces, and adaptive stealth technologies.

Environmental concerns and regulatory pressures (e.g., Restriction of Hazardous Substances, RoHS) are indirectly driving the need for eco-friendly absorber synthesis. This includes replacing toxic organic solvents with water-based systems (as demonstrated by Bobsin *et al*. using aqueous graphene/CMC suspensions), utilizing bio-derived or renewable feedstocks (e.g., cellulose, lignin, chitosan), and minimizing energy consumption through low-temperature, ambient-pressure processes [69]. As electronics manufacturing moves toward net-zero emissions, circular economy principles will become increasingly important.

The Mechanisms of Multi-Physics Synergy and Multifunctional Integration Remain Unclear. Current research predominantly focuses on the optimization of individual electromagnetic performance, leading to an insufficient understanding of the multi-physics coupling behavior of absorbing materials under the actual service conditions within integrated circuits. The dynamic evolution of electromagnetic parameters under coupled conditions such as high temperature, high frequency, and thermal cycling remains ambiguous, and systematic studies on the synergistic mechanisms between absorption performance, thermal management, and mechanical reliability are lacking. Furthermore, the thermo-mechanical-electrical coupling behavior at the interfaces between the absorbing material and dissimilar materials—such as chips, packaging substrates, and heat spreaders—requires urgent in-depth investigation, and interfacial failure mechanisms along with lifetime prediction models have yet to be established. Future efforts should focus on constructing multi-physics coupling simulation platforms to investigate the performance degradation mechanisms of absorbing materials under extreme environments [110, 111]. The development of multifunctional composites that integrate absorption, thermal conduction, and stress buffering capabilities is essential to achieve an integrated "absorption-packaging-thermal dissipation" design. The research

and development of absorbing materials for integrated circuits offers a transformative technological pathway for chip-level electromagnetic protection. However, its comprehensive advancement remains contingent upon synergistic innovation across multiple disciplines, including materials science, microelectronics processing, electromagnetic field theory, and thermodynamics. In the future, through deep interdisciplinary integration, with an emphasis on intelligent design, lightweight integration, and dynamic tunability, it is anticipated that existing technical bottlenecks can be overcome, providing core support for the stable operation of next-generation high-performance integrated circuits.

REFERENCES

[1] Jiang IR-H, Chang Y-W, Huang J-L, Chen C-P. Intelligent design automation for 2.5/3D heterogeneous SoC integration. In: Proceedings of the 39th International Conference on Computer-Aided Design. 2020:1-7. https://doi.org/10.1145/3400302.3415732

[2] Kazior TE. Beyond CMOS: heterogeneous integration of III–V devices, RF MEMS and other dissimilar materials/devices with Si CMOS to create intelligent microsystems. Philos Trans R Soc A Math Phys Eng Sci. 2014;372(2012). https://doi.org/10.1098/rsta.2013.0105

[3] Sun N, Liu M. Integrated chips: An interdisciplinary evolution in the Post-Moore Era. Fundam Res. 2024;4(6):1405. https://doi.org/10.1016/j.fmre.2024.05.015

[4] Liu X, Kamineni S, Breiholz J, Calhoun BH, Li S. A sub-μW energy-performance-aware IoT SoC with a triple-mode power management unit for system performance scaling, fast DVFS, and energy minimization. IEEE J Solid-State Circuits. 2024;59(7):2272-2285. https://doi.org/10.1109/JSSC.2024.3356789

[5] Jia F, Lu Z, Huang T, Xu M, Xu X, Guo Z, *et al*. Twin-coated skeleton PEDOT:PSS/MXene/para-aramid nanofibers hybrid aerogel with efficient EMI shielding performance and tunable power coefficient. Adv Compos Hybrid Mater. 2025;8(2):1-17. https://doi.org/10.1007/s42114-025-01234-5

[6] Hareesh MS, Joseph P, George S. Electromagnetic interference shielding: a comprehensive review of materials, mechanisms, and applications. Nanoscale Adv. 2025;7(15):4510-4534. https://doi.org/10.1039/D5NA00234K

[7] Wang L, Cheng J, Zou Y, Zheng W, Wang Y, Liu Y, *et al*. Current advances and future perspectives of MXene-based electromagnetic interference shielding materials. Adv Compos Hybrid Mater. 2023;6(5):172. https://doi.org/10.1007/s42114-023-00748-0

[8] Iwasaki N, Katsura K, Kukutsu N. Wideband package using an electromagnetic absorber. Electron Lett. 1993;29(10):875-876. https://doi.org/10.1049/el:19930586

[9] Moon K, Wong CP, Kim S, Choi HD, Han S, Yoon HG, *et al*. Ferrite polymer composite for improving the electromagnetic compatibility of semiconductor packaging. J Electron Mater. 2007;36(12):1711-1718. https://doi.org/10.1007/s11664-007-0276-9

[10] Ding B, Wang Y, Li Y, Jiang H, Guo J, Sun Y, *et al*. Lightweight, core-shell structured regenerated silk fibroin/MXene nanofiber composite film for efficient electromagnetic wave absorption in the X-band. Mater Today Commun. 2025:113632. https://doi.org/10.1016/j.mtcomm.2025.113632

[11] Li H, Li H, Sheng B, Zheng B, Shi S, Cai Q, *et al*. Synthesis of cobalt particles and investigation of their electromagnetic wave absorption characteristics. Materials. 2023;17(1):200. https://doi.org/10.3390/ma17010200

[12] Choudhary A, Pal S, Sarkhel G. Broadband millimeter-wave absorbers: a review. Int J Microw Wirel Technol. 2023;15(2):347-363. https://doi.org/10.1017/S1759078722000457

[13] Qu N, Sun H, Sun Y, He M, Xing R, Gu J, *et al*. 2D/2D coupled MOF/Fe composite metamaterials enable robust ultra–broadband microwave absorption. Nat Commun. 2024;15(1):5642. https://doi.org/10.1038/s41467-024-49892-1

[14] Praful P, Bailey C. Warpage in wafer-level packaging: a review of causes, modelling, and mitigation strategies. Front Electron. 2025;5:1515860. https://doi.org/10.3389/felec.2024.1515860

[15] Hubing TH, Beetner DG, Deng S, Dong X. Radiation mechanisms for semiconductor devices and packages. In: Proceedings of the 2004 International Symposium on Electromagnetic Compatibility; 2004; Santa Clara, CA.

[16] Lee D, Lee J-Y, Lee K, Kim M, Kim M, Youn Y, *et al*. Design, fabrication, and far-field measurement of FOWLP-based tightly coupled antenna modules integrated with CMOS chipset for mmWave applications. In: 2023 IEEE/MTT-S International Microwave Symposium - IMS 2023. IEEE; 2023:478-481. https://doi.org/10.1109/IMS37964.2023.10188122

[17] Wu K-B, Kuo T-Y, Hung C-C, Lin B, Peng I-H, Yang M-T, *et al*. Novel RDL design of wafer-level packaging for signal/power integrity in LPDDR4 application. IEEE Trans Compon Packag Manuf Technol. 2018;8(8):1431-1439. https://doi.org/10.1109/TCPMT.2018.2829905

[18] Liu Z, Jiang H, Zhu Z, Chen L, Sun Q, Zhang W. Crosstalk noise of octagonal TSV array arrangement based on different input signal. Processes. 2022;10(2):260. https://doi.org/10.3390/pr10020260

[19] Wang Y, Liu H, Huo L, Li H, Tian W, Ji H, *et al*. Research on the reliability of advanced packaging under multi-field coupling: a review. Micromachines. 2024;15(4):422. https://doi.org/10.3390/mi15040422

[20] Chandrakar M, Majumder MK. Impact of a tubular dielectric medium on peak noise and crosstalk delay in a coaxial TSV. In: Emerging Electronic Devices, Circuits and Systems. Springer; 2023:191-208. https://doi.org/10.1007/978-981-19-1779-8_14

[21] Joung BK, Kim S-C, Ahn K-O, Kim Y-H. Electromagnetic interference shielding from the back-side metallization of the chip in fan-out wafer level package. J Nanoelectron Optoelectron. 2021;16(5):723-730. https://doi.org/10.1166/jno.2021.3030

[22] Liu X, Sun Q, Huang Y, Chen Z, Liu G, Zhang DW. Optimization of TSV leakage in via-middle TSV process for wafer-level packaging. Electronics. 2021;10(19):2370. https://doi.org/10.3390/electronics10192370

[23] Kim Y, Park G, Cho K, Raj PM, Tummala RR, Kim J. Wideband power/ground noise suppression in low-loss glass interposers using a double-sided electromagnetic bandgap structure. IEEE Trans Microw Theory Tech. 2020;68(12):5055-5064. https://doi.org/10.1109/TMTT.2020.3026820

[24] Wang H, Ma J, Yang Y, Gong M, Wang Q. A review of system-in-package technologies: application and reliability of advanced packaging. Micromachines. 2023;14(6):1149. https://doi.org/10.3390/mi14061149

[25] Braun T, Becker K-F, Hoelck O, Kahle R, Woehrmann M, Toepper M, *et al*. Fan-out wafer level packaging for 5G and mm-Wave applications. In: 2018 International Conference on Electronics Packaging and iMAPS All Asia Conference (ICEP-IAAC). IEEE; 2018:247-251. https://doi.org/10.23919/ICEP.2018.8374332

[26] Tsai M-H, Hsu S-K, Shen C-K, Wei P-S, Chern C-H, Wu T-L. A miniature electromagnetic bandgap structure using integrated fan-out wafer-level package (InFO-WLP) for gigahertz noise suppression. In: 2018 IEEE/MTT-S International Microwave Symposium - IMS. IEEE; 2018:1542-1544. https://doi.org/10.1109/MWSYM.2018.8439410

[27] Li Y, Shen Z. Integrated circuit heterogeneous manufacturing technology. In: 2025 International Conference on Electronics, Electrical and Grid Technology (ICEEGT 2025). Atlantis Press; 2026:109-119. https://doi.org/10.2991/978-94-6463-458-5_13

[28] Xia Q, Zhang X, Ma B, Tao K, Zhang H, Yuan W, *et al*. A state-of-the-art review of through-silicon vias: filling materials, filling processes, performance, and integration. Adv Eng Mater. 2025;27(1):2401799. https://doi.org/10.1002/adem.202401799

[29] Fan Y, Zhou Y, Wang Q, Lei B, Song G, Zhang W, *et al*. Design and verification of silicon bridge in 2.5D advanced package based on universal chiplet interconnect express (UCIe). Microelectron Reliab. 2025;168:115710. https://doi.org/10.1016/j.microrel.2025.115710

[30] Han KJ, Lim Y, Kim Y. A performance analysis for interconnections of 3D ICs with frequency-dependent TSV model in s-parameter. J Semicond Technol Sci. 2014;14(5):649-657. https://doi.org/10.5573/JSTS.2014.14.5.649

[31] Qian L-B, Zhu Z-M, Xia Y-S, Ding R-X, Yang Y-T. Through-silicon-via crosstalk model and optimization design for three-dimensional integrated circuits. Chin Phys B. 2014;23(3):038402. https://doi.org/10.1088/1674-1056/23/3/038402

[32] Zhao K, An Y, Sun X, Miao M, Li Z, Zhao Y. Characterization of corner/edge effects of through silicon via arrays and layout optimization in 3D integrated circuits. Jpn J Appl Phys. 2021;60(SB):SBBC05. https://doi.org/10.35848/1347-4065/abe155

[33] Ndip I, Curran B, Lobbicke K, Guttowski S, Reichl H, Lang K-D, *et al*. High-frequency modeling of TSVs for 3-D chip integration and silicon interposers considering skin-effect, dielectric quasi-TEM and slow-wave modes. IEEE Trans Compon Packag Manuf Technol. 2011;1(10):1627-1641. https://doi.org/10.1109/TCPMT.2011.2162840

[34] Oh H, Thadesar PA, May GS, Bakir MS. Low-loss air-isolated through-silicon vias for silicon interposers. IEEE Microw Wirel Compon Lett. 2016;26(3):168-170. https://doi.org/10.1109/LMWC.2016.2524529

[35] Pal K, Halavar B, Kumar VR. Design of silicon core coaxial TSVs to reduce crosstalk effects for 3D IC applications. IETE J Res. 2024;70(12):8656-8662. https://doi.org/10.1080/03772063.2024.2357560

[36] Yi H, Zhu J, Fan J, Wang D, Mao J. Through-silicon via advanced packaging technology and its radio frequency applications. Chip. 2025:100158. https://doi.org/10.1016/j.chip.2025.100158

[37] Cho K, Kim Y, Lee H, Song J, Park J, Lee S, *et al*. Signal integrity design and analysis of differential high-speed serial links in silicon interposer with through-silicon via. IEEE Trans Compon Packag Manuf Technol. 2018;9(1):107-121. https://doi.org/10.1109/TCPMT.2018.2883108

[38] Yang D-C, Xie J, Swaminathan M, Wei X-C, Li E-P. A rigorous model for through-silicon vias with ohmic contact in silicon interposer. IEEE Microw Wirel Compon Lett. 2013;23(8):385-387. https://doi.org/10.1109/LMWC.2013.2270781

[39] Shiba K, Kosuge A, Hamada M, Kuroda T. Crosstalk analysis and countermeasures of high-bandwidth 3D-stacked memory using multi-hop inductive coupling interface. IEICE Trans Electron. 2023;106(7):391-394. https://doi.org/10.1587/transele.2022ECP5027

[40] Sicard E, Wu J, Shen R, Li E-P, Liu E-X, Kim J, *et al*. Recent advances in electromagnetic compatibility of 3D-ICs—Part II. IEEE Electromagn Compat Mag. 2016;5(1):65-74. https://doi.org/10.1109/MEMC.2016.7497955

[41] Garnier A, Castagné L, Gréco F, Guillemet T, Maréchal L, Neffati M, *et al*. System in package embedding III-V chips by fan-out wafer-level packaging for RF applications. In: 2021 IEEE 71st Electronic Components and Technology Conference (ECTC). IEEE; 2021:2016-2023. https://doi.org/10.1109/ECTC32696.2021.00317

[42] Li Y, Pan B, Ge Z, Chen P, Bi B, Yi X, *et al*. Soldering and bonding in contemporary electronic device packaging. Materials. 2025;18(9):2015. https://doi.org/10.3390/ma18092015

[43] Jiang R, Uehling T, He B, Zhou T, Song M, Sukemi AM, *et al*. Semiconductor chip and package co-design and assembly for dual use in flip chip and wirebond BGA packages. In: 2024 IEEE 26th Electronics Packaging Technology Conference (EPTC). IEEE; 2024:207-213. https://doi.org/10.1109/EPTC62928.2024.10840020

[44] Nobert G, Constantin NG, Blaquière Y. GHz-range modeling of power integrity in an array of simultaneously switching power converters. IEEE Trans Electromagn Compat. 2024;67(1):316-327. https://doi.org/10.1109/TEMC.2024.3498321

[45] Sasaki H, Govind V, Srinivasan K, Dalmia S, Sundaram V, Swaminathan M, *et al*. Electromagnetic interference (EMI) issues for mixed-signal system-on-package (SOP). In: 2004 Proceedings 54th Electronic Components and Technology Conference. IEEE; 2004:1437-1442. https://doi.org/10.1109/ECTC.2004.1320340

[46] Bharath K, Engin E, Swaminathan M, Uriu K, Yamada T. Signal and power integrity co-simulation for multi-layered system on package modules. In: 2007 IEEE International Symposium on Electromagnetic Compatibility. IEEE; 2007:1-6. https://doi.org/10.1109/ISEMC.2007.170

[47] Shim Y, Park J, Kim J, Song E, Yoo J, Pak J, *et al*. Modeling and analysis of simultaneous switching noise coupling for a CMOS negative-feedback operational amplifier in system-in-package. IEEE Trans Electromagn Compat. 2009;51(3):763-773. https://doi.org/10.1109/TEMC.2009.2024378

[48] Azuma N, Nagata M. Equivalent circuit representation of silicon substrate coupling of passive and active RF components. IEICE Trans Electron. 2013;96(6):875-883. https://doi.org/10.1587/transele.E96.C.875

[49] Kuroda T, Miura N. Perspective of low-power and high-speed wireless inter-chip communications for SiP integration. In: 2006 European Solid-State Device Research Conference. IEEE; 2006:3-6. https://doi.org/10.1109/ESSDER.2006.307628

[50] Arnaudov RG. Evaluation of via shielding on parasitic coupling, cavity-resonance modes, and radiation in multilayer packages. J Microelectron Electron Packag. 2009;6(3):172-181. https://doi.org/10.4071/1551-4897-6.3.172

[51] Abbas SM, Chandra M, Verma A, Chatterjee R, Goel TC. Complex permittivity and microwave absorption properties of a composite dielectric absorber. Compos Part A Appl Sci Manuf. 2006;37(11):2148-2154. https://doi.org/10.1016/j.compositesa.2005.11.009

[52] Zhang X, Wang Q, Tang Y, Fan G, Hao C, Liu Y. Decoration of conjugated polyacene quinone radical (PAQR) with Fe_3O_4 nanospheres achieving improved impedance matching and electromagnetic wave absorption. Mater Today Phys. 2024;41:101349. https://doi.org/10.1016/j.mtphys.2024.101349

[53] Hou Z-L, Gao X, Zhang J, Wang G. A perspective on impedance matching and resonance absorption mechanism for electromagnetic wave absorbing. Carbon. 2024;222:118935. https://doi.org/10.1016/j.carbon.2024.118935

[54] Park S-H, Ahn W-K, Kum J-S, Ji J-K, Kim K-H, Seong W-M. Electromagnetic properties of dielectric and magnetic composite material for antenna. Electron Mater Lett. 2009;5(2):67-71. https://doi.org/10.3365/eml.2009.06.067

[55] Li C, Li D, Zhang S, Ma L, Zhang L, Zhang J, *et al*. Interface engineering of titanium nitride nanotube composites for excellent microwave absorption at elevated temperature. Nano-Micro Lett. 2024;16(1):168. https://doi.org/10.1007/s40820-024-01340-9

[56] Zhang K, Yan Y, Wang Z, Ma G, Jia D, Huang X, *et al*. Integration of electrical properties and polarization loss

modulation on atomic Fe–N-RGO for boosting electromagnetic wave absorption. Nano-Micro Lett. 2025;17(1):46. https://doi.org/10.1007/s40820-024-01523-4

[57] Bao W, Liu Y, Zhao X. Recent research progress of carbon-based and their composites for electromagnetic waves absorption. Text Res J. 2023;93(7-8):1889-1912. https://doi.org/10.1177/00405175221134717

[58] Chen G, Li Z, Zhang L, Chang Q, Chen X, Fan X, *et al*. Mechanisms, design, and fabrication strategies for emerging electromagnetic wave-absorbing materials. Cell Rep Phys Sci. 2024;5(7). https://doi.org/10.1016/j.xcrp.2024.102013

[59] Mohammed I, Mohammed J, Srivastava AK. Recent progress in hexagonal ferrites based composites for microwave absorption. Cryst Res Technol. 2023;58(3):2200200. https://doi.org/10.1002/crat.202200200

[60] Darwish KA, Hemeda OM, Abdel Ati MI, Abd El-Hameed AS, Zhou D, Darwish MA, *et al*. Synthesis, characterization, and electromagnetic properties of polypyrrole–barium hexaferrite composites for EMI shielding applications. Appl Phys A. 2023;129(6):460. https://doi.org/10.1007/s00339-023-06755-8

[61] Siddiki SH, Riscob B, Ajay K, Maity CK, Sahoo S. Dielectric loss-driven microwave absorbing materials. Coord Chem Rev. 2026;551:217471. https://doi.org/10.1016/j.ccr.2025.217471

[62] Zhou Y, He P, Ma W, Zuo P, Xu J, Tang C, *et al*. The developed wave cancellation theory contributing to understand wave absorption mechanism of ZIF derivatives with controllable electromagnetic parameters. Small. 2024;20(2):2305277. https://doi.org/10.1002/smll.202305277

[63] Fante RL, McCormack MT. Reflection properties of the Salisbury screen. IEEE Trans Antennas Propag. 1988;36(10):1443-1454. https://doi.org/10.1109/8.8632

[64] He M, Zhang K, Qiu H, Guo H, Li X, Guo Y, *et al*. Low-frequency microwave absorption composites. Adv Sci. 2025;12(35):e11580. https://doi.org/10.1002/advs.202511580

[65] Venugopal V, Kumar BS, Kurup DG, Thota SM. Advances in microwave absorbing and shielding materials: the role of zero-dimensional carbon nanoparticles. Mater Technol. 2025;40(1):2496318. https://doi.org/10.1080/10667857.2025.2496318

[66] Li Z, Chen X, Liu D, Zhou Y, Pan D, Shin S. Recent advances in polymer-based composites for thermal management and electromagnetic wave absorption. Adv Compos Hybrid Mater. 2025;8(2):210. https://doi.org/10.1007/s42114-025-01245-2

[67] Ma J, Wang J, Hu X, Wang L, Fan Y, Jiang W. Construction of plate-like magnetic heterostructure for synergistic microwave absorption. J Am Ceram Soc. 2023;106(1):410-419. https://doi.org/10.1111/jace.18845

[68] Zhao R, Gao T, Li Y, Sun Z, Zhang Z, Ji L, *et al*. Highly anisotropic Fe_3C microflakes constructed by solid-state phase transformation for efficient microwave absorption. Nat Commun. 2024;15(1):1497. https://doi.org/10.1038/s41467-024-45829-w

[69] Bobsin A, Kerber RM, Fernandes IJ, Ferreira SB, Hasenkamp W, Peter CR, *et al*. Conductive water-based graphene suspension for electromagnetic interference shielding via spray coating on SiP module. Prog Org Coat. 2024;195:108658. https://doi.org/10.1016/j.porgcoat.2024.108658

[70] Niu Q, Huang Y, Huang H, Zong M. A flexible and repairable ultra-broadband electromagnetic wave absorber by liquid-liquid phase separation strategy. Adv Mater. 2025;e10139. https://doi.org/10.1002/adma.202510139

[71] Zhang R, Ye X, Tan S, Wang Y, Li R, He E, *et al*. $(CoCrFeCuNi)_3O_4$@C-graphene/PLA composite material exhibits thin, wide-bandwidth, and excellent microwave absorption properties. Ceram Int. 2025. https://doi.org/10.1016/j.ceramint.2025.01.405

[72] Shu J, Zhou J, Cao B, Lu S, Ding D, Zi Z. Magneto-dielectric synergy design $CoFe_2O_4$ decorated MXene composites for broadband electromagnetic wave absorption. Diam Relat Mater. 2025;113041. https://doi.org/10.1016/j.diamond.2025.113041

[73] Zheng H, Nan K, Lu Z, Wang N, Wang Y. Core-shell FeCo@carbon nanocages encapsulated in biomass-derived carbon aerogel: architecture design and interface engineering of lightweight, anti-corrosion and superior microwave absorption. J Colloid Interface Sci. 2023;646:555-566. https://doi.org/10.1016/j.jcis.2023.05.062

[74] Liang J, Ye F, Cao Y, Mo R, Cheng L, Song Q. Defect-engineered graphene/Si3N4 multilayer alternating core-shell nanowire membrane: a plainified hybrid for broadband electromagnetic wave absorption. Adv Funct Mater. 2022;32(22):2200141. https://doi.org/10.1002/adfm.202200141

[75] Liu P, He Z, Li X, Ding L, Liu S, Kong J. Multifunctional hollow carbon microspheres enable superior electromagnetic wave response and corrosion barrier. Adv Mater. 2025;37(35):2500646. https://doi.org/10.1002/adma.202500646

[76] Wang K, Zhou Q, Li W. Conductive metal-organic frameworks for electromagnetic wave absorption. Chin J Struct Chem. 2024;43(10):100325. https://doi.org/10.1016/j.cjsc.2024.100325

[77] Zhang Y, Tian Y, Xu N, Cui P, Guo L, Ma J, *et al*. In situ mechanical foaming of hierarchical porous MoC for assembling ultra-light, self-cleaning, heat-insulation, flame-retardant, and infrared-stealth device. Adv Funct Mater. 2025;35(6):2414910. https://doi.org/10.1002/adfm.202414910

[78] Qi J, Liang C, Ruan K, Li M, Guo H, He M, *et al*. Cactus-like architecture for synergistic microwave absorption and thermal management. Natl Sci Rev. 2025;nwaf394. https://doi.org/10.1093/nsr/nwaf394

[79] Zhang Y, Pan L, Zhang P, Sun Z. Gradient multilayer design of $Ti_3C_2T_x$ MXene nanocomposite for strong and broadband microwave absorption. Small Sci. 2022;2(7):2200018. https://doi.org/10.1002/smsc.202200018

[80] Xie K, Zhang Q, Chen F, Fu Q. Enhanced ultra-broadband electromagnetic wave absorption using liquid metal-coated carbonyl Fe/Ni microspheres with dual dielectric polarization. J Mater Chem C. 2025;13(14):7167-7178. https://doi.org/10.1039/D5TC00345B

[81] Luu MD, Luu TN, Le TH, Tran QD, Pham SH, Nguyen TG, *et al*. Defect-interface synergy in lightweight Fe_3O_4/rGO@SiO_2 nanocomposite for broadband electromagnetic wave absorption. Mater Sci Eng B. 2026;324:119023. https://doi.org/10.1016/j.mseb.2025.119023

[82] Liu P, Huang L, Zheng C, Bao Y, Gao D, Zhou G. Spin coating in semiconductor lithography: advances in modeling and future prospects. Microelectron Eng. 2025;298:112326. https://doi.org/10.1016/j.mee.2025.112326

[83] Langen A, Senes A, de Vries I, Groen P. Bead behavior in a non-continues slot die coating regime.

[84] Li J, Wang C, Miao T, Guo S, Tong Y, Zhang L. Airflow-assisted acoustic spray coating for suppressing pinhole defects on photoresist film. Mater Sci Semicond Process. 2025;196:109657. https://doi.org/10.1016/j.mssp.2025.109657

[85] Lee S, Tiara AM, Cho G, Lee J. Control of the drying patterns for complex colloidal solutions and their applications. Nanomaterials. 2022;12(15):2600. https://doi.org/10.3390/nano12152600

[86] Tadros TF. Polymeric surfactants: dispersion stability and industrial applications. Walter de Gruyter GmbH & Co KG; 2017.

[87] Ding H, Hu B, Wang Y, Du Y. Current progress and frontiers in three-dimensional macroporous carbon-based aerogels for

electromagnetic wave absorption: a review. Nanoscale. 2024;16(47):21731-21760. https://doi.org/10.1039/D4NR03624K

[88] Hao Y, Leng Z, Yu C, Xie P, Meng S, Zhou L, *et al*. Ultra-lightweight hollow bowl-like carbon as microwave absorber owning broad band and low filler loading. Carbon. 2023;212:118156. https://doi.org/10.1016/j.carbon.2023.118156

[89] Ren S, Yu H, Wang L, Huang Z, Lin T, Huang Y, *et al*. State of the art and prospects in metal-organic framework-derived microwave absorption materials. Nano-Micro Lett. 2022;14(1):68. https://doi.org/10.1007/s40820-022-00805-z

[90] Fang Z-Q, Mao C, Wu J-M, Shi Z-A, Yang S-L, Chen Y, *et al*. Fabrication of Cf/SiC wave absorbing materials with high dielectric loss by powder bed fusion (PBF) combined with chemical vapor reaction (CVR) method. Ceram Int. 2025;51(12):15818-15829. https://doi.org/10.1016/j.ceramint.2025.01.123

[91] Liu Q, Hai W, Li M, Chen N, Shao G, Shao H, *et al*. Synthesis of hierarchical SiC@MA@Ni heterostructure fibers via MXene-reduced Ag NPs activator and electroless Ni deposition for electromagnetic microwaves absorption. Appl Mater Today. 2026;48:102997. https://doi.org/10.1016/j.apmt.2025.102997

[92] Liu L, Yibibulla T, Yang Y, Hassan SU, Hou L, Kuang D, *et al*. Design and microwave absorption characteristics of porous lamellar hard carbon materials. Microporous Mesoporous Mater. 2024;369:113041. https://doi.org/10.1016/j.micromeso.2024.113041

[93] Chen Z, Zhou J, Fu X, Jiang H, Zhang X, Yao J, *et al*. Effect of different morphologies induced by in situ semi-conversion strategy on MOF-derived microwave absorbers. Chem Eng J. 2023;474:145917. https://doi.org/10.1016/j.cej.2023.145917

[94] He P, Ma W, Xu J, Wei J, Liu X, Zuo P, *et al*. Induced crystallization-controllable nanoarchitectonics of 3D-ordered hierarchical macroporous Co@N-doped carbon frameworks for enhanced microwave absorption. Small. 2023;19(1):2204649. https://doi.org/10.1002/smll.202204649

[95] Liu P, Gao S, Zhang G, Huang Y, You W, Che R. Hollow engineering to Co@N-doped carbon nanocages via synergistic protecting-etching strategy for ultrahigh microwave absorption. Adv Funct Mater. 2021;31(27):2102812. https://doi.org/10.1002/adfm.202102812

[96] Peng H, Zhang D, Xie Z, Lu S, Liu Y, Liang F. Recent advances in structural design of carbon/magnetic composites and their electromagnetic wave absorption applications. Small. 2025;21(8):2408570. https://doi.org/10.1002/smll.202408570

[97] Deng L, Zhao X, Wei X, Sun Q, Xu J. Machine learning-aided optimization of 3D-printed MWCNTs/NiFe/PETG osteospermum stepped-structure via full-wave simulation for broadband microwave absorption. J Alloys Compd. 2025;185182. https://doi.org/10.1016/j.jallcom.2025.185182

[98] Yang C, He E, Yang P, Gao Q, Yan T, Ye X, *et al*. 3D-printed stepped structure based on graphene-FeSiAl composites for broadband and wide-angle electromagnetic wave absorption. Compos Part B Eng. 2024;270:111135. https://doi.org/10.1016/j.compositesb.2023.111135

[99] Wang W, Li Z, Gao X, Huang Y, He R. Material extrusion 3D printing of large-scale SiC honeycomb metastructure for ultra-broadband and high temperature electromagnetic wave absorption. Addit Manuf. 2024;85:104158. https://doi.org/10.1016/j.addma.2024.104158

[100] Yin L, Tian X, Cui C, Wang Z. A bioinspired helical metamaterial for broadband electromagnetic wave absorption. Compos Part B Eng. 2025;112685. https://doi.org/10.1016/j.compositesb.2025.112685

[101] Li C, Wang Q, Cui Y, Wang L, Yang Z. Digital light processing of 3D-printable all-dielectric metamaterial absorbers based on reduced graphene oxide@Fe_3O_4 and reduced graphene oxide@Fe_3O_4@MoS_2 composites. J Alloys Compd. 2025;185118. https://doi.org/10.1016/j.jallcom.2025.185118

[102] Huo S, Li Y, Lei X, Sun Z, Yu H, Li B, *et al*. Analysis of a novel resistive film absorber for suppression of electromagnetic radiation in system-in-packages. Int J Antennas Propag. 2022;2022(1):7674970. https://doi.org/10.1155/2022/7674970

[103] Liu Z, Wang Y, Xian C, Li K, Wang F, Zhang P, *et al*. High-performance microwave absorbers using a simple double-layer absorbing structure to improve impedance mismatching. J Alloys Compd. 2023;938:168649. https://doi.org/10.1016/j.jallcom.2022.168649

[104] Huang Z, Wan L, Tian J, Sun Z, Ahmad M, Wu J, *et al*. NC@TiO_2 microwave-absorber microspheres: control of shell thickness and evaluation of electromagnetic performance. Carbon. 2025;243:120511. https://doi.org/10.1016/j.carbon.2025.120511

[105] Liu J, Dong J, Tang M, Si Y, Wang Y, Sun R. Research progress on the microwave absorbers with core–shell micro-structure design. Mater Des. 2025;114420. https://doi.org/10.1016/j.matdes.2025.114420

[106] He Z, Sun R, Xu H, Geng W, Liu P. Metal-organic-frameworks derived hollow carbon derivatives: controllable configurations and optimized microwave absorption. Carbon. 2024;219:118853. https://doi.org/10.1016/j.carbon.2024.118853

[107] Qi Q, Li T, Yang H, Lv A, Liu Y, Meng F. Recent advances in structural engineering of ceramic microwave absorption materials: from nano/micro architectures to macroscale design. J Adv Ceram. 2025. https://doi.org/10.26599/JAC.2025.9221043

[108] Le Saos A, Ville J, Laur V, Maalouf A, Chevalier A, Roquefort P, *et al*. Influence of particle geometry and polymer matrix composition on filament processing, rheological and electromagnetic properties: towards 3D printable composites for microwave absorption. Mater Sci Eng B. 2025;317:118167. https://doi.org/10.1016/j.mseb.2025.118167

[109] Tilve-Martínez D, Neri W, Lessire J, Dulucq B, Vukadinovic N, Berton B, *et al*. Ultralow UV absorber content in 3D printed nanocomposites: maximizing printability and microwave absorption efficiency. J Phys Mater. 2025;8(1):015010. https://doi.org/10.1088/2515-7639/ad8f2a

[110] Lu Z, Liu L, Chen Z, Wang C, Zhu X, Lu X, *et al*. Progress in electromagnetic wave absorption of multifunctional structured metamaterials. Polymers. 2025;17(18):2559. https://doi.org/10.3390/polym17182559

[111] Wang R, He M, Zhou Y, Nie S, Wang Y, Liu W, *et al*. Metal-organic frameworks self-templated cubic hollow Co/N/C@MnO_2 composites for electromagnetic wave absorption. Carbon. 2020;156:378-388. https://doi.org/10.1016/j.carbon.2019.09.063

https://doi.org/10.66000/3110-9772.2026.02.02